

A Distance Geometry Protocol to Generate Conformations of Natural Products to Structurally Interpret Ion Mobility-Mass Spectrometry Collision Cross Sections

Sarah M. Stow,^{1,3,4} Cody R. Goodwin,^{1,3,4} Michal Kliman,^{1,3,4} Brian O. Bachmann,^{1,3}
John A. McLean,^{1,3,4} and Terry P. Lybrand^{1,2,3,5}

(1) Department of Chemistry, (2) Department of Pharmacology, (3) Vanderbilt Institute of Chemical Biology, (4) Vanderbilt Institute of Integrative Biosystems Research Education, (5) Center for Structural Biology, Vanderbilt University, Nashville, TN 37235

Corresponding Authors:

Terry P. Lybrand (Phone: 615.343.1247; Email: terry.p.lybrand@vanderbilt.edu) and
John A. McLean (Phone: 615.322.1195; Email: john.a.mclean@vanderbilt.edu)

Abstract:

Ion mobility-mass spectrometry (IM-MS) allows the separation of ionized molecules based on their charge-to-surface area (IM) and mass-to-charge ratio (MS), respectively. The IM drift time data that is obtained is used to calculate the ion-neutral collision cross section (CCS) of the ionized molecule with the neutral drift gas, which is directly related to the ion conformation and hence molecular size and shape. Studying the conformational landscape of these ionized molecules computationally provides interpretation to delineate the potential structures that these CCS values could represent, or conversely, structural motifs not consistent with the IM data. A challenge in the IM-MS community is the ability to rapidly compute conformations to interpret natural product data, a class of molecules exhibiting a broad range of biological activity. The diversity of biological activity is, in part, related to the unique structural characteristics often observed for natural products. Contemporary approaches to structurally interpret IM-MS data for peptides and proteins typically utilize molecular dynamics (MD) simulations to sample conformational space. However, MD calculations are computationally expensive, they require a force field that accurately describes the molecule of interest, and there is no simple metric that indicates when sufficient conformational sampling has been achieved. Distance geometry is a computationally inexpensive approach that creates conformations based on sampling different pair-wise distances between the atoms within the molecule and therefore does not require a force field. Progressively larger distance bounds can be used in distance geometry calculations, providing in principle a strategy to assess when all plausible conformations have been sampled. Our results suggest that distance geometry is a computationally efficient and potentially superior strategy for conformational analysis of natural products to interpret gas-phase CCS data.

Table of Contents

Protocol Details and Performance Data	Pages 3-4
Clustering Data	Pages 5-14
Conformational Space Plot Comparison	Page 15-16
Ion Mobility Trace with Sample Structures	Page 17
QM Geometry Optimization Conformational Space Plots	Page 18
Conformational Space Plots for Distance Geometry with 2,000 Structures	Page 19
Sample Conformations	Pages 20-40
Clustering Data of Conformations	Pages 41-48

Table S-1. Structural information concerning the 10 natural products used in this study. Number of atoms, number of rotatable bonds, number of oxygens, number of chiral centers, and number of double bonds.

Molecule	# of atoms	# of rotatable bonds	# of oxygens	# of chiral centers	# of double bonds
Brefeldin	44	0	4	5	2
Ampicillin	43	5	4	4	0
Doxorubicin	68	5	11	6	0
Capsaicin	49	10	3	0	1
Lincomycin	61	8	6	9	0
Neomycin	88	9	13	19	0
Josamycin	127	14	15	16	2
Erythromycin	118	7	13	18	0
Antimycin	79	14	9	4	0
Valinomycin	168	9	18	12	0

Table S-2. Number of structures that are generated with each method as well as the number of structures plotted after 1.0 RMSD clustering cutoff.

Molecule	# of structures generated when 20,000 requested	# of structures generated when 8,000 requested	# of structures used from 8,000 DG	# of structures used from SA	# of structures after 1.0 RMSD clustering for 8,000DG	# of structures after 1.0 RMSD clustering for SA
Brefeldin	15	15	15	3000	7	31
Ampicillin	282	268	268	3000	36	22
Doxorubicin	314	307	307	3000	152	111
Capsaicin	2864	2736	2736	9000	805	1336
Lincomycin	10995	8000	7997	9000	2580	301
Neomycin	20000	8000	8000	9000	7175	2255
Josamycin	20000	8000	7797	9000	7726	3105
Erythromycin	20000	8000	7982	9000	7509	857
Antimycin	20000	8000	7995	9000	4657	2036
Valinomycin	20000	8000	8000	9000	8000	7546

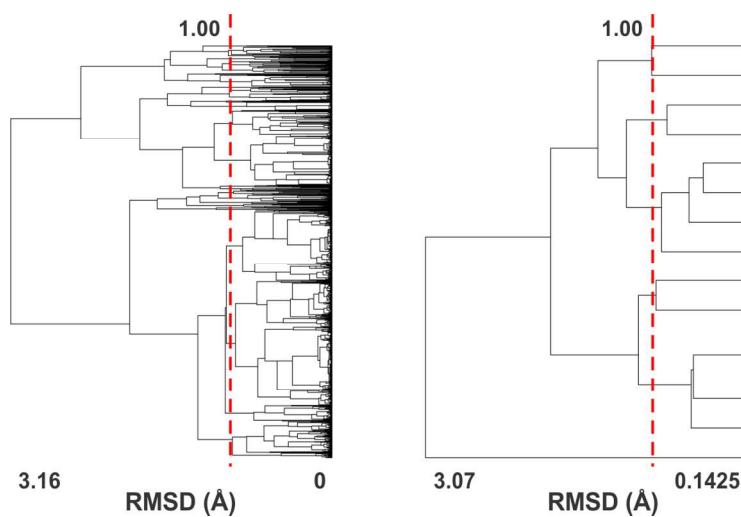


Figure S-1. Clustering analysis for brefeldin for a) simulated annealing, and b) distance geometry. The vertical bar indicates the RMSD cutoff (1.0 Å) used to select a comparable number of structures from both methods.

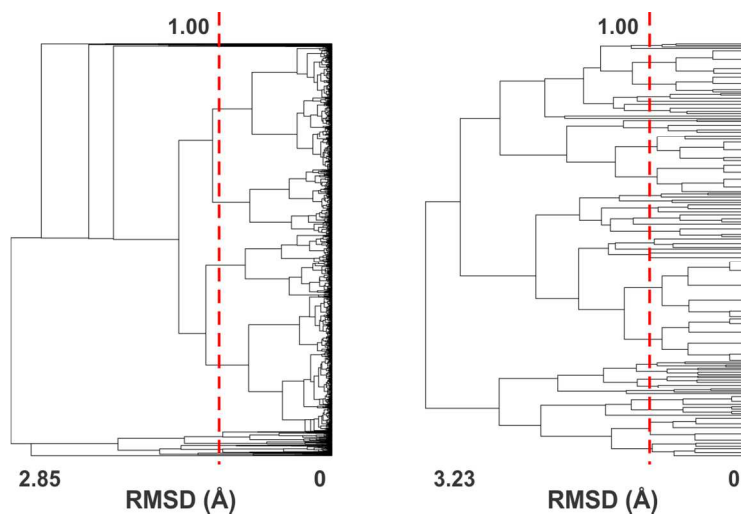


Figure S-2. Clustering analysis for ampicillin for a) simulated annealing, and b) distance geometry. The vertical bar indicates the RMSD cutoff (1.0 Å) used to select a comparable number of structures from both methods.

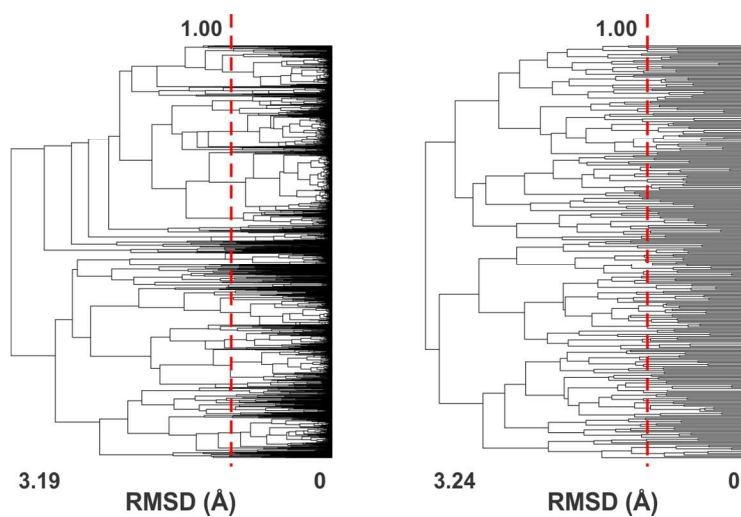


Figure S-3. Clustering analysis for doxorubicin for a) simulated annealing, and b) distance geometry. The vertical bar indicates the RMSD cutoff (1.0 Å) used to select a comparable number of structures from both methods.

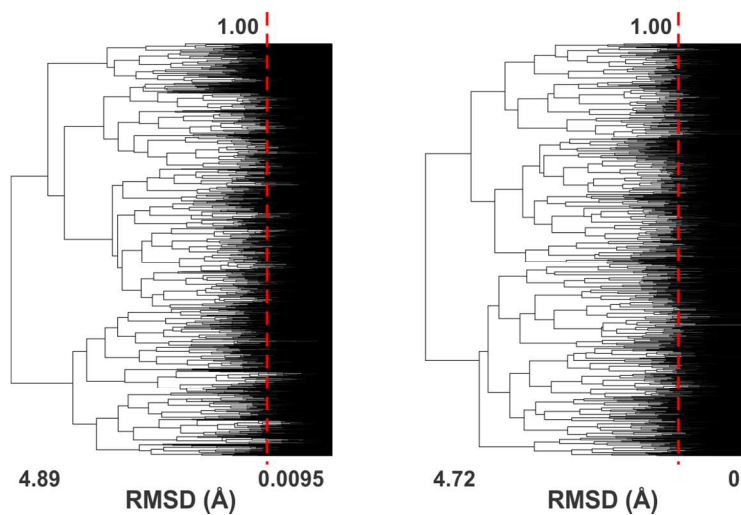


Figure S-4. Clustering analysis for capsaicin for a) simulated annealing, and b) distance geometry. The vertical bar indicates the RMSD cutoff (1.0 Å) used to select a comparable number of structures from both methods.

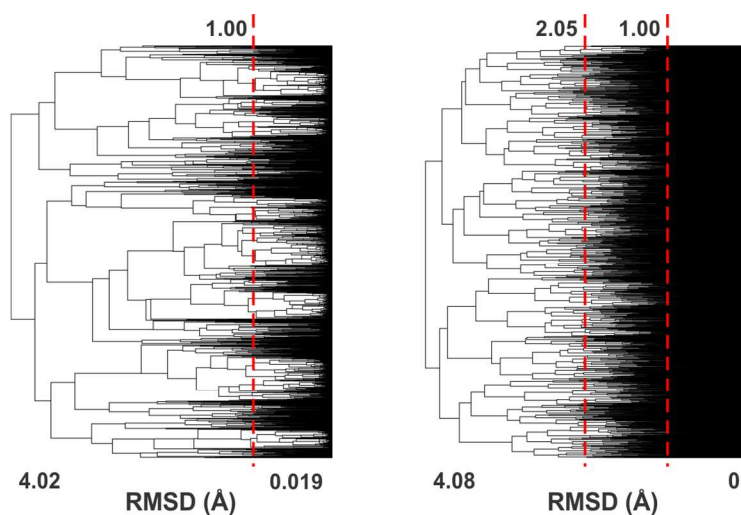


Figure S-5. Clustering analysis for lincomycin for a) simulated annealing, and b) distance geometry. The vertical bar at 1.0 Å indicates the RMSD cutoff used to select a comparable number of structures from both methods. The other vertical bar at 2.05 Å indicates the RMSD cutoff for the QM geometry optimization.

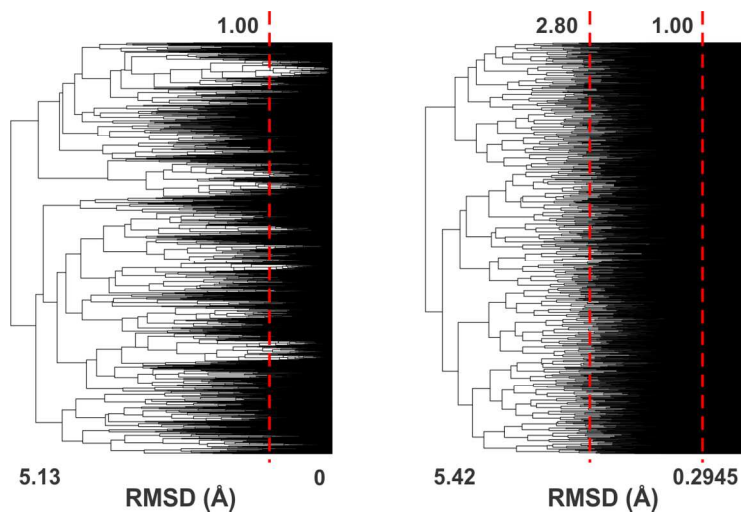


Figure S-6. Clustering analysis for neomycin for a) simulated annealing, and b) distance geometry. The vertical bar at 1.0 Å indicates the RMSD cutoff used to select a comparable number of structures from both methods. The other vertical bar at 2.80 Å indicates the RMSD cutoff for the QM geometry optimization.

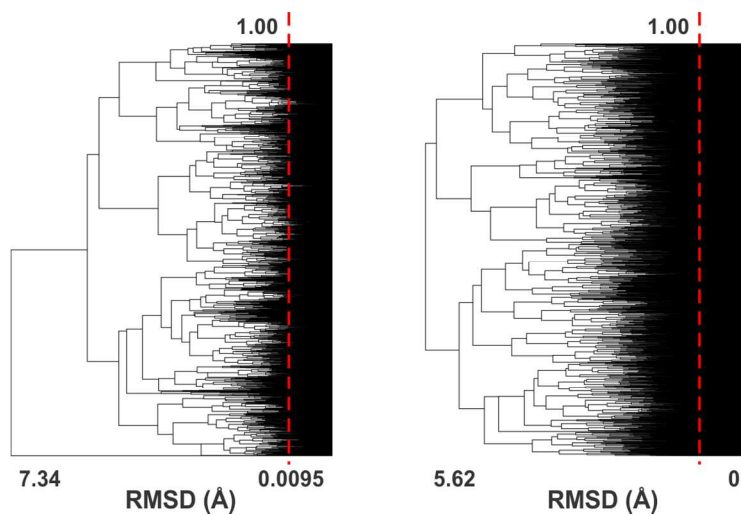


Figure S-7. Clustering analysis for antimycin for a) simulated annealing and b) distance geometry. The vertical bar indicates the RMSD cutoff (1.0 Å) used to select a comparable number of structures from both methods.

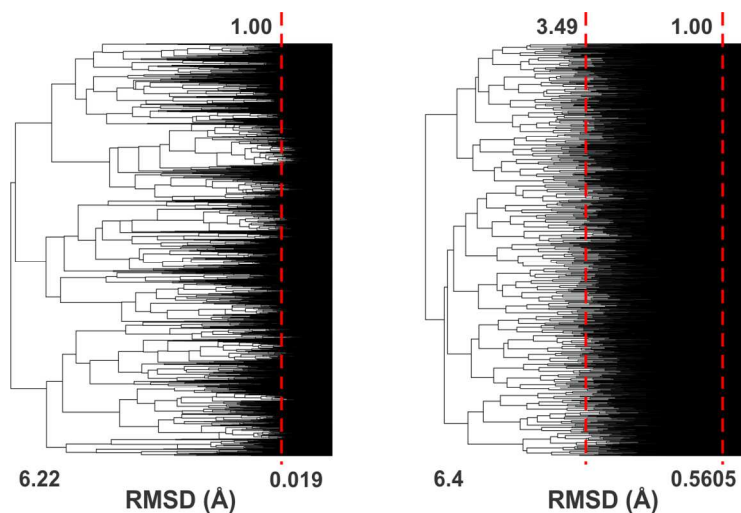


Figure S-8. Clustering analysis for josamycin for a) simulated annealing and b) distance geometry. The vertical bar at 1.0 Å indicates the RMSD cutoff used to select a comparable number of structures from both methods. The other vertical bar at 3.49 Å indicates the RMSD cutoff for the QM geometry optimization.

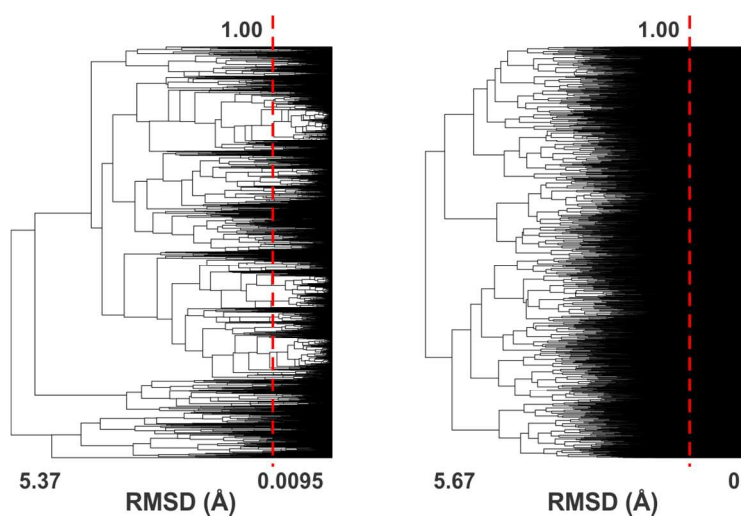


Figure S-9. Clustering analysis for erythromycin for a) simulated annealing, and b) distance geometry. The vertical bar indicates the RMSD cutoff (1.0 Å) used to select a comparable number of structures from both methods.

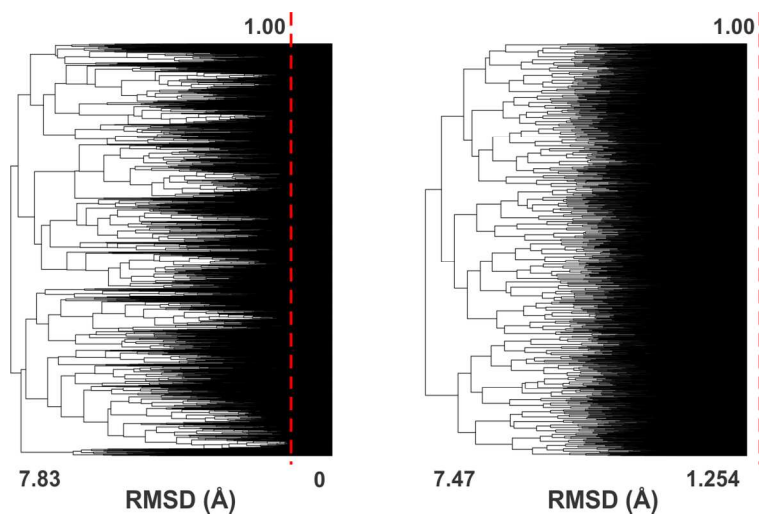


Figure S-10. Clustering analysis for valinomycin for a) simulated annealing, and b) distance geometry. The vertical bar indicates the RMSD cutoff (1.0 Å) used to select a comparable number of structures from both methods.

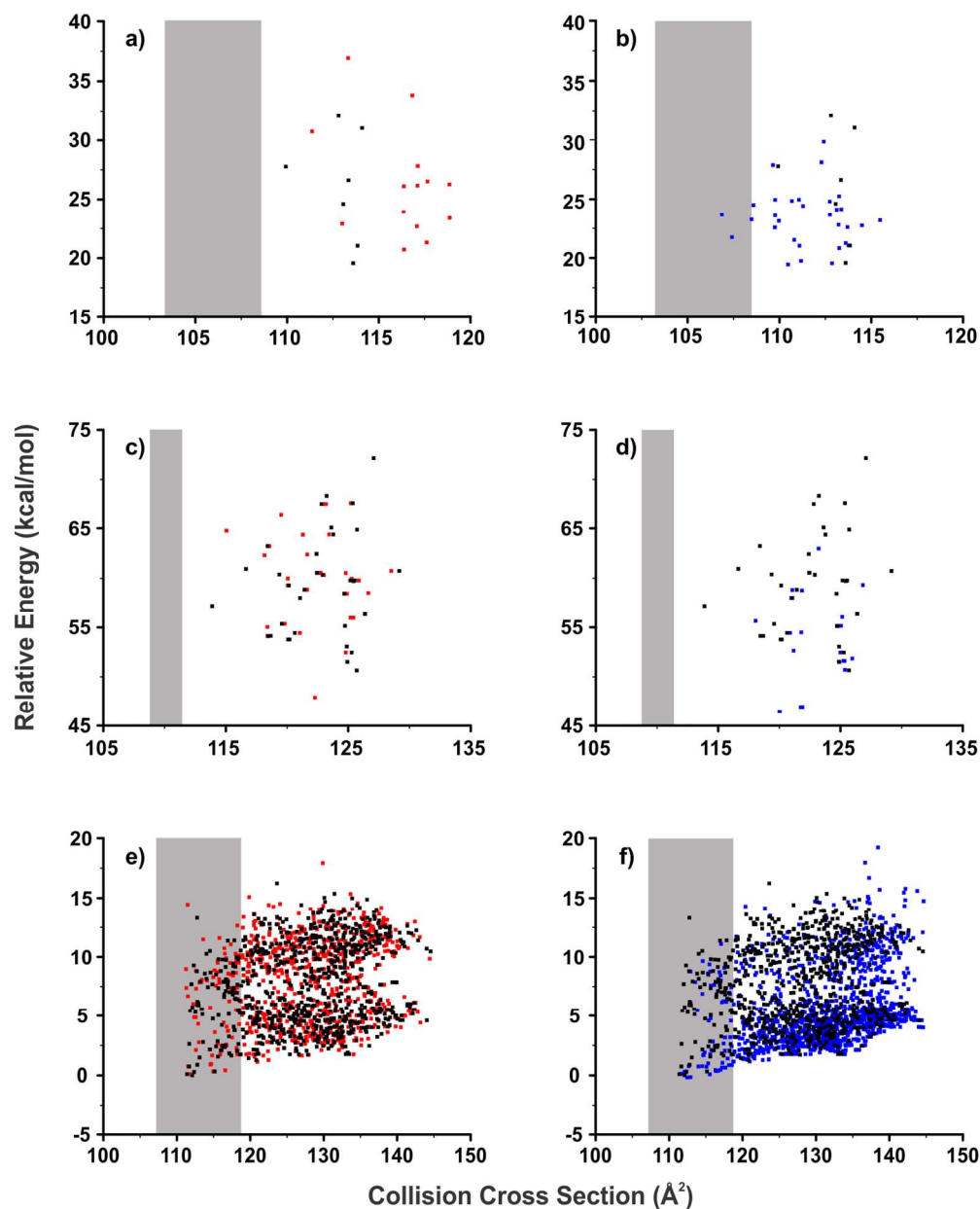


Figure S-11. Conformational space plots for three of the natural products: a,b) brefeldin, c,d) ampicillin, and e,f) capsaicin. The panel on the left shows distance geometry results when 20,000 (red) or 8,000 (black) initial structures are requested from the calculation. The panel on the right compares the distance geometry results (8,000 conformations are requested) to simulated annealing results (blue). The grey vertical bar indicated the experimental CCS range. Note that for brefeldin the distance geometry fails to generate conformations as small as the experimental range determined by IM-MS, and for ampicillin neither distance geometry nor MD-based conformational sampling generates any conformations consistent with the experimental CCS data. This most likely reflects small errors for both the experimental measurements and theoretical calculations, which is not surprising for molecules of this size (where the relative contribution of long range interaction potentials to CCS increases) under the experimental and theoretical methods presented in this manuscript.

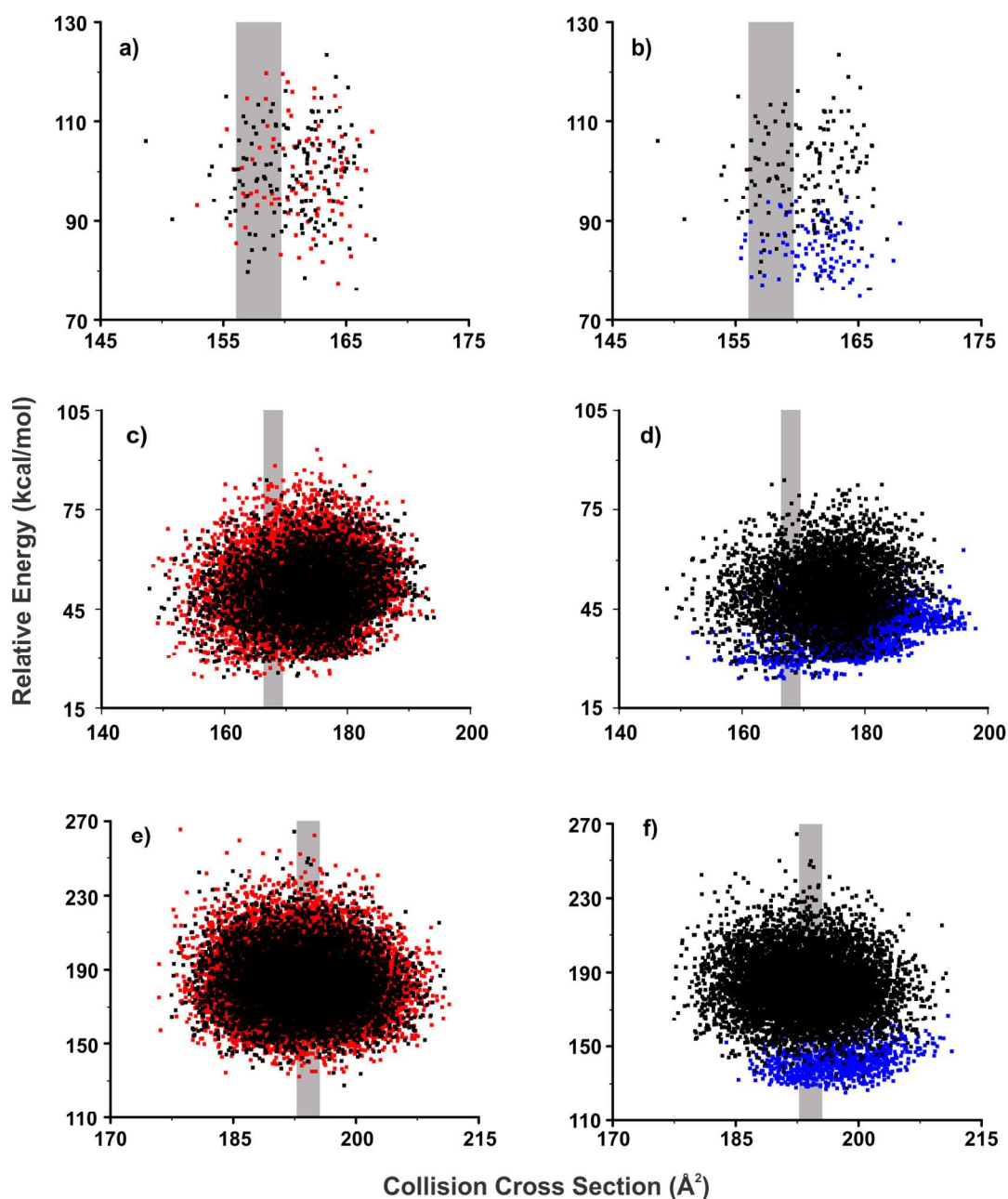


Figure S-12. Conformational space plots for three of the natural products: a,b) doxorubicin, c,d) antimycin, and e,f) erythromycin. The panel on the left shows distance geometry results when 20,000 (red) or 8,000 (black) initial structures are requested from the calculation. The panel on the right compares the distance geometry results (8,000 conformations are requested) to simulated annealing results (blue). The grey vertical bar indicated the experimental CCS range.

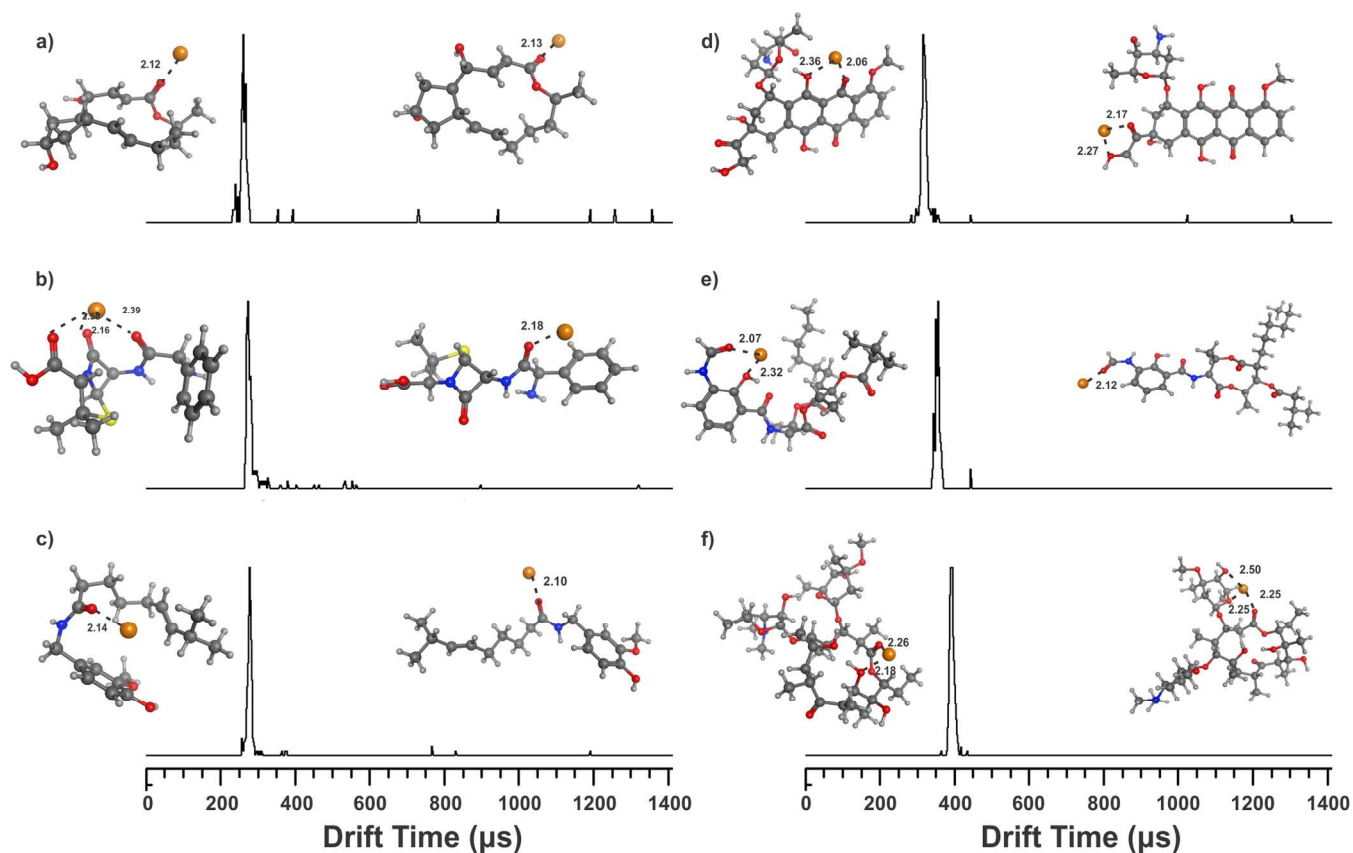


Figure S-13. IM traces for the representative natural products, namely (a) brefeldin, (b) ampicillin, (c) capsaicin, (d) doxorubicin, (e) antimycin, and (f) erythromycin. The most representative conformation generated with distance geometry from within the experimental range is shown to the left of the mobility peak and a conformation that does not agree with the experimental measurement is shown on the right of the mobility peak to illustrate the coordination of computation with experiment for interpretation of structure.

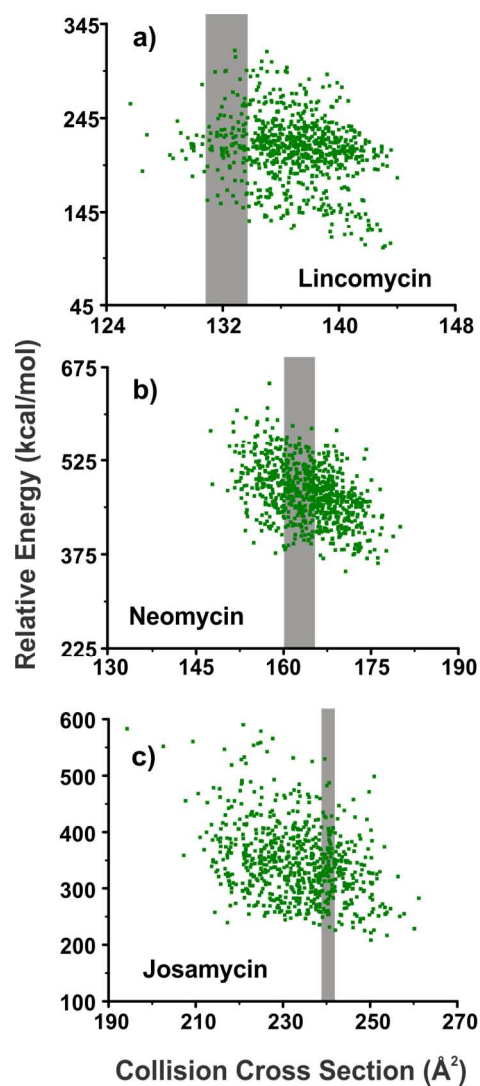


Figure S-14. Conformational space plots for three of the natural products: a) lincomycin, b) neomycin, and c) josamycin when distance geometry is performed with the Gaussian09 QM geometry optimization. The theoretical CCS value is plotted against the relative theoretical energy. The grey vertical bar indicated the experimental CCS range.

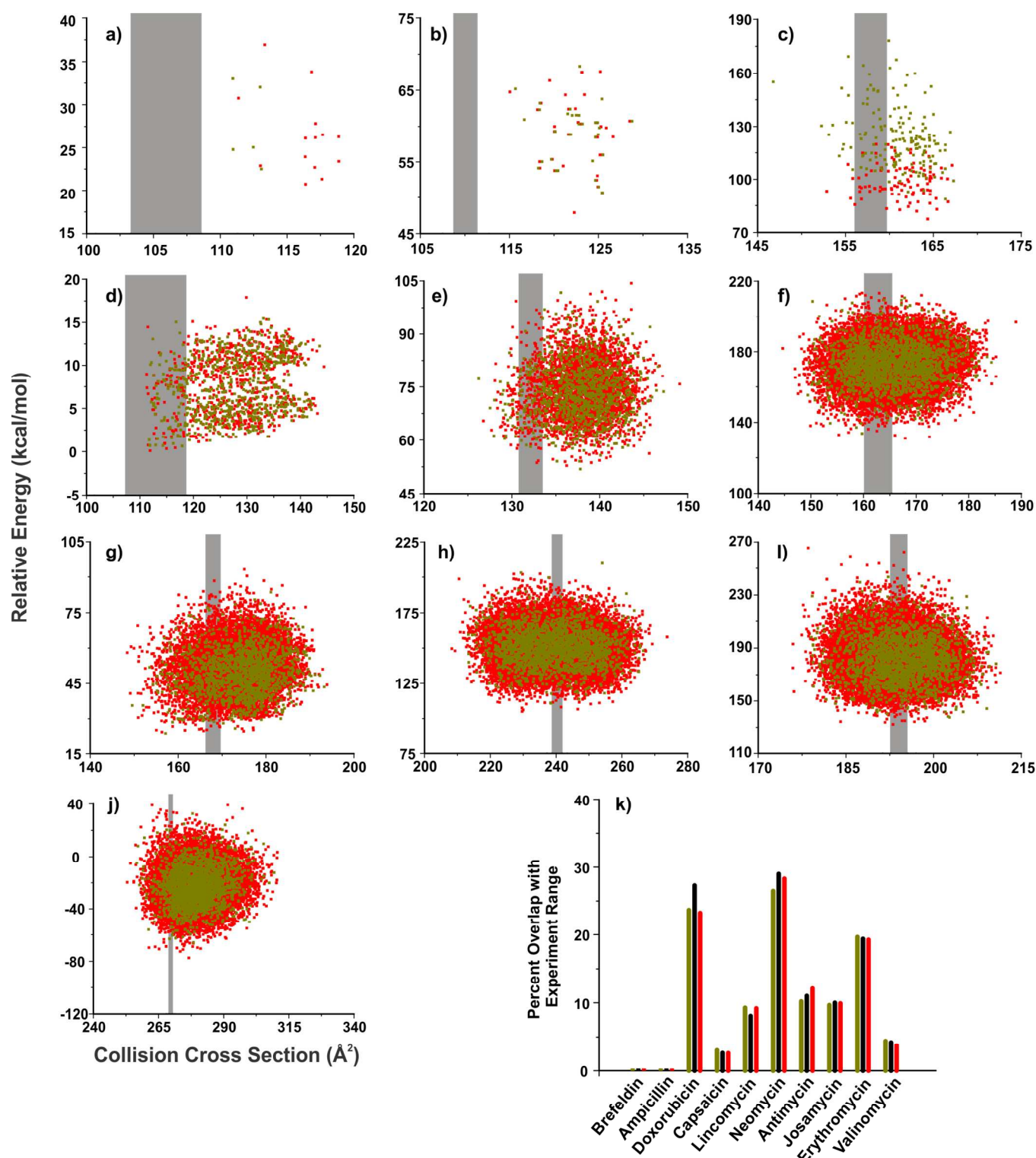


Figure S-15. Conformational space plots for the ten natural products: a) brefeldin, b) ampicillin, c) doxorubicin, d) capsaicin, e) lincomycin, f) neomycin, g) antimycin, h) josamycin, i) erythromycin, and j) valinomycin. In k) the percent of generated conformations within the experimental range is shown. The results for 20,000 conformations are shown in red, for 8,000 in black, and for 2,000 in gold.

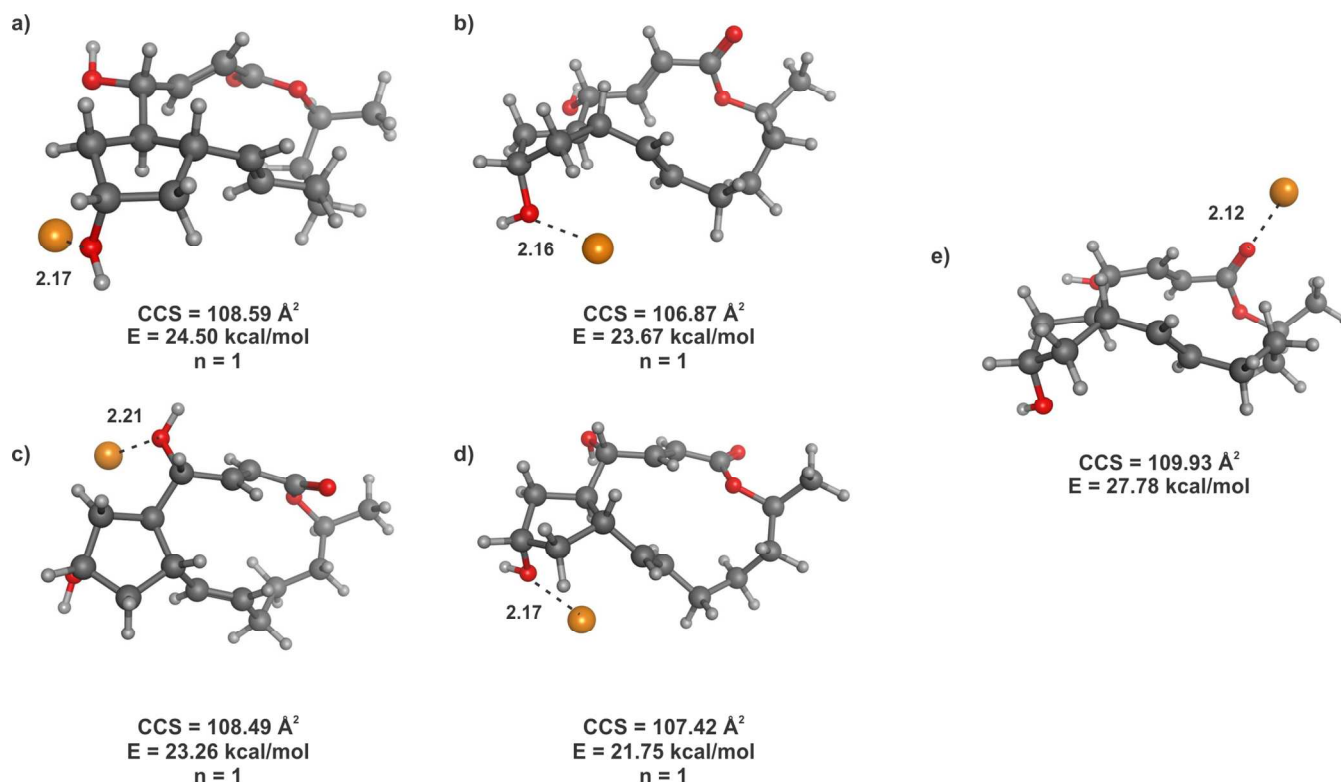


Figure S-16. Representative conformations of brefeldin generated with both simulated annealing and distance geometry. The conformations shown in a-d) were generated with simulated annealing and are the four conformations that fall within the experimental CCS range. For distance geometry, none of the generated conformations fall within the experimental range. The conformation shown in e) is the conformation with the closest theoretical CCS to the experimental range. Each conformation is labeled with its theoretical CCS value and its theoretical energy. Carbon atoms are shown in dark grey, hydrogen in light grey, oxygen in red, nitrogen in blue, sulfur in yellow, and sodium in orange. Each conformation is labeled with its theoretical CCS value and its theoretical energy. All the conformations generated with distance geometry coordinate the cation at the carbonyl oxygen, which is the most electronegative oxygen according to the electrostatic potential that introduces the sodium cation. The short energy minimization that follows the introduction of the cation is not long enough to allow the sodium cation to sample further conformational space. The conformations that have the sodium cation coordinated to the carbonyl oxygen represent larger CCS values that do not align with the experimental measurements.

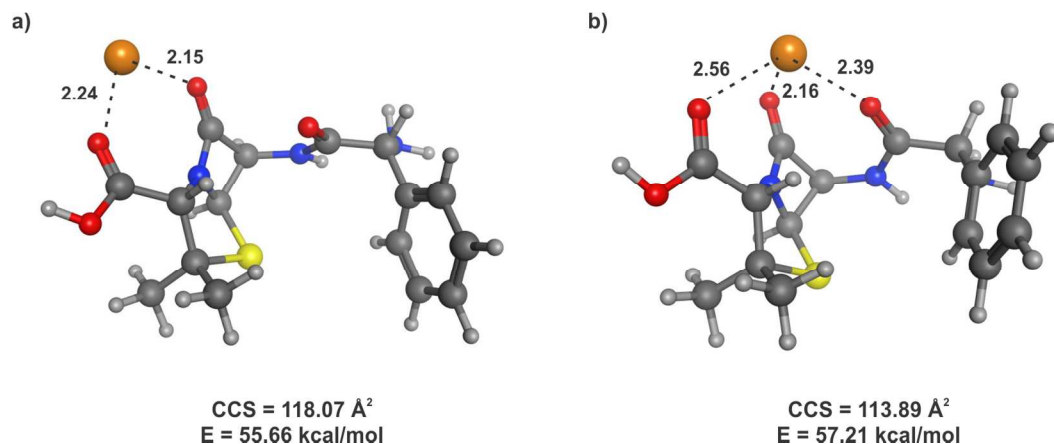


Figure S-17. Representative conformations of ampicillin generated with a) simulated annealing and b) distance geometry. Clustering data is not shown for ampicillin because none of the generated conformations aligned with the experimental CCS value. These conformations had theoretical CCS values that most closely aligned with the experimental CCS value. Carbon atoms are shown in dark grey, hydrogen in light grey, oxygen in red, nitrogen in blue, sulfur in yellow, and sodium in orange. Each conformation is labeled with its theoretical CCS value and its theoretical energy. The lack of overlap with experimental data is most likely representative of experimental conditions that were not optimized for molecules of this size.

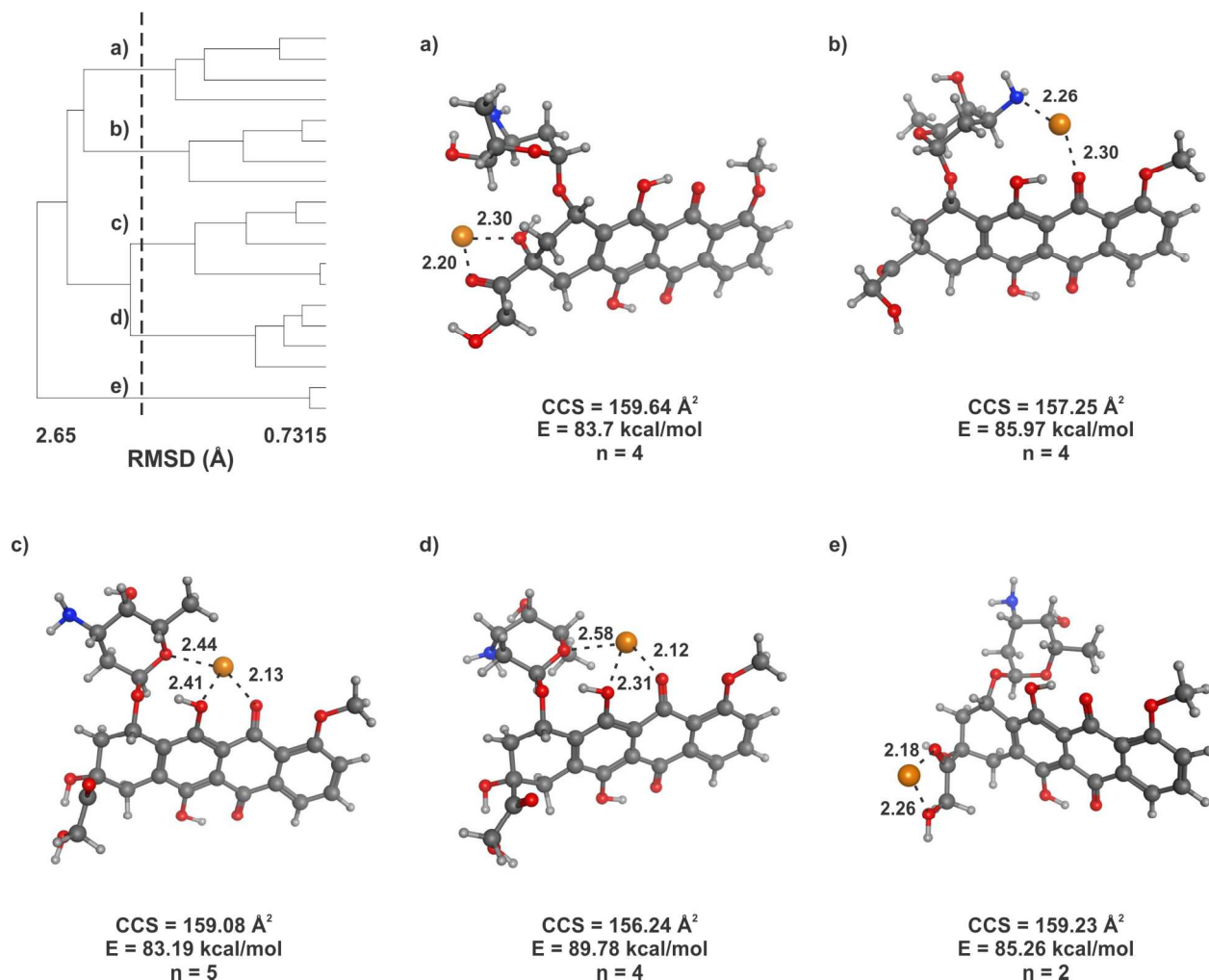


Figure S-18. Clustering analysis of 19 conformations of doxorubicin generated with simulated annealing that fall within the experimental CCS range. Clustering is based on root mean square distance of atoms of superimposed structures. The vertical bar indicates the RMSD cutoff (1.81 Å) used to select the shown conformations. The conformations indicated on the clustering tree are shown with corresponding letters. Carbon atoms are shown in dark grey, hydrogen in light grey, oxygen in red, nitrogen in blue, and sodium in orange. Each conformation is labeled with its theoretical CCS value, its theoretical energy, and the number of conformations it represents from the clustering analysis.

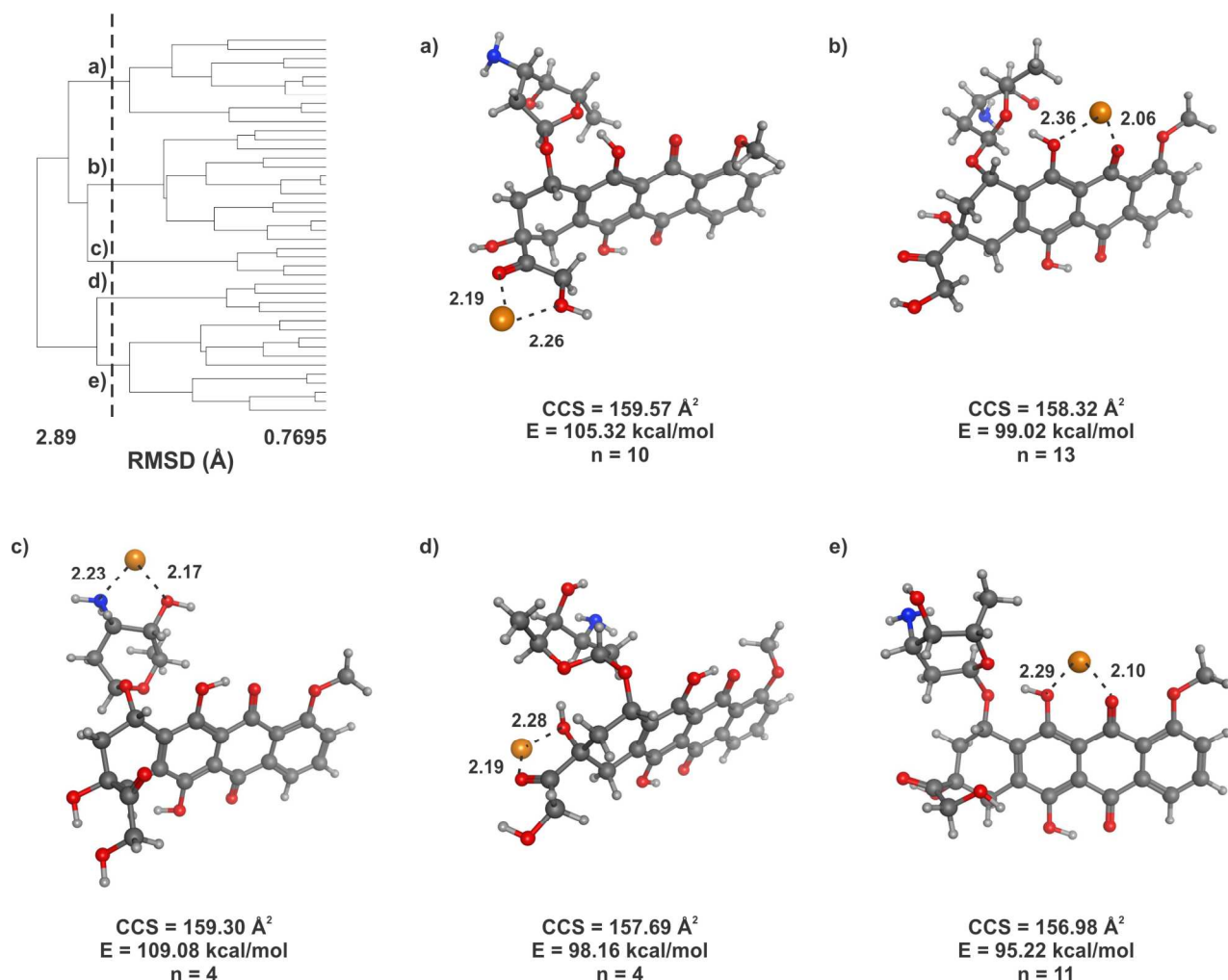


Figure S-19. Clustering analysis of 42 conformations of doxorubicin generated with distance geometry that fall within the experimental CCS range. Clustering is based on root mean square distance of atoms of superimposed structures. The vertical bar indicates the RMSD cutoff (2.40 Å) used to select the shown conformations. The conformations indicated on the clustering tree are shown with corresponding letters. Carbon atoms are shown in dark grey, hydrogen in light grey, oxygen in red, nitrogen in blue, and sodium in orange. Each conformation is labeled with its theoretical CCS value, its theoretical energy, and the number of conformations it represents from the clustering analysis.

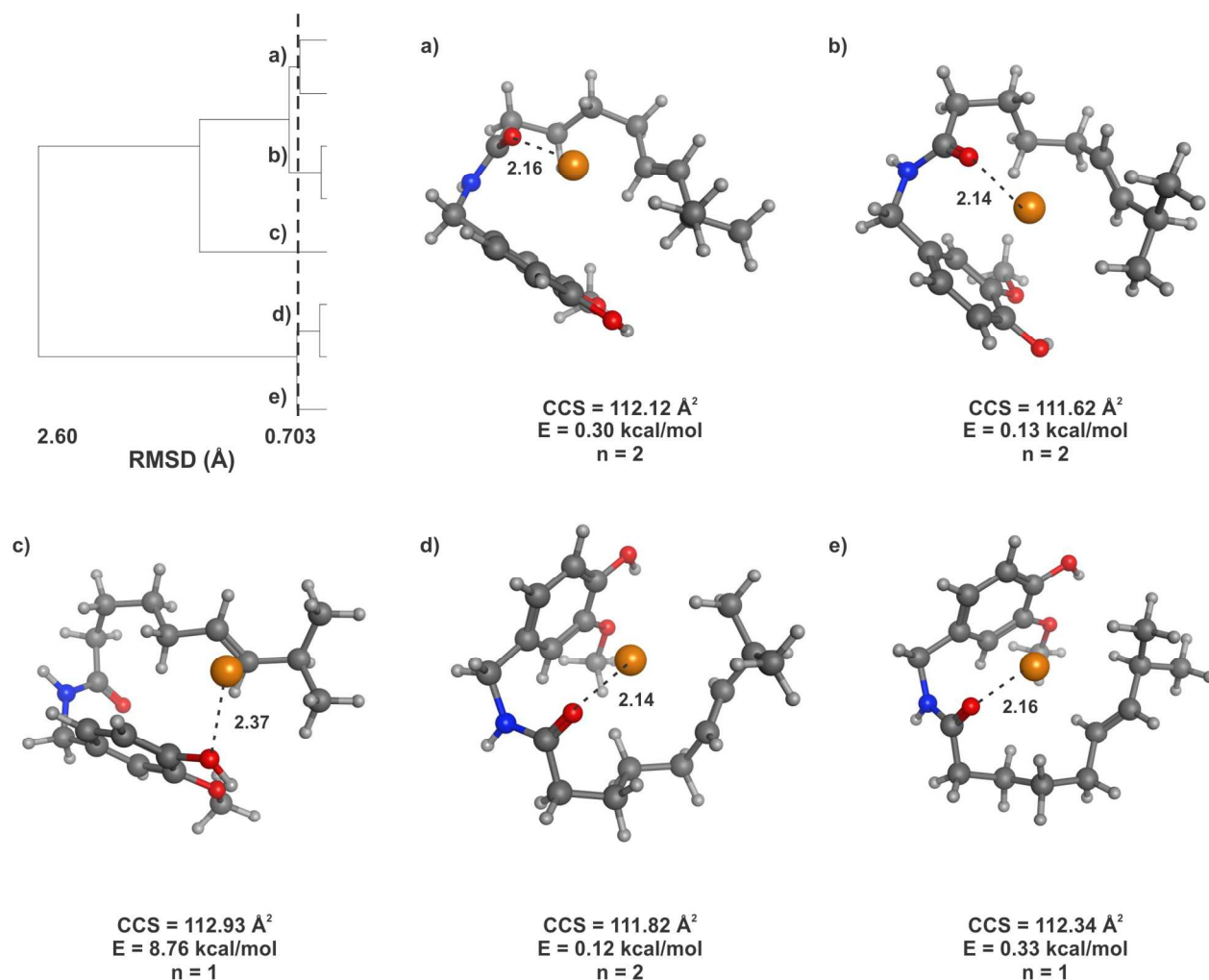


Figure S-20. Clustering analysis of 8 conformations of capsaicin generated with simulated annealing that fall within the experimental CCS range. Clustering is based on root mean square distance of atoms of superimposed structures. The vertical bar indicates the RMSD cutoff (0.89 Å) used to select the shown conformations. The conformations indicated on the clustering tree are shown with corresponding letters. Carbon atoms are shown in dark grey, hydrogen in light grey, oxygen in red, nitrogen in blue, and sodium in orange. Each conformation is labeled with its theoretical CCS value, its theoretical energy, and the number of conformations it represents from the clustering analysis.

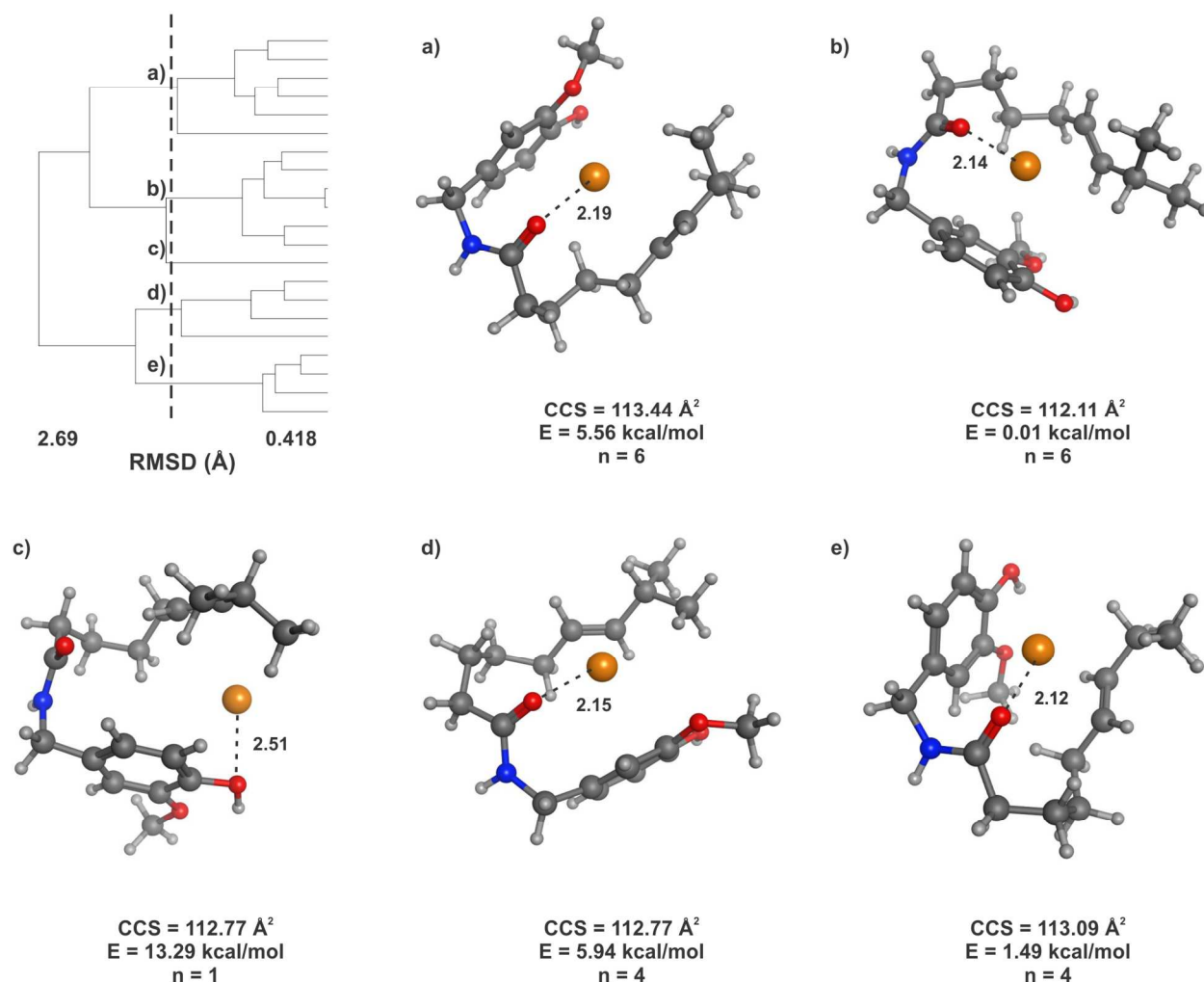


Figure S-21. Clustering analysis of 21 conformations of capsaicin generated with distance geometry that fall within the experimental CCS range. Clustering is based on root mean square distance of atoms of superimposed structures. The vertical bar indicates the RMSD cutoff (1.60 Å) used to select the shown conformations. The conformations indicated on the clustering tree are shown with corresponding letters. Carbon atoms are shown in dark grey, hydrogen in light grey, oxygen in red, nitrogen in blue, and sodium in orange. Each conformation is labeled with its theoretical CCS value, its theoretical energy, and the number of conformations it represents from the clustering analysis.

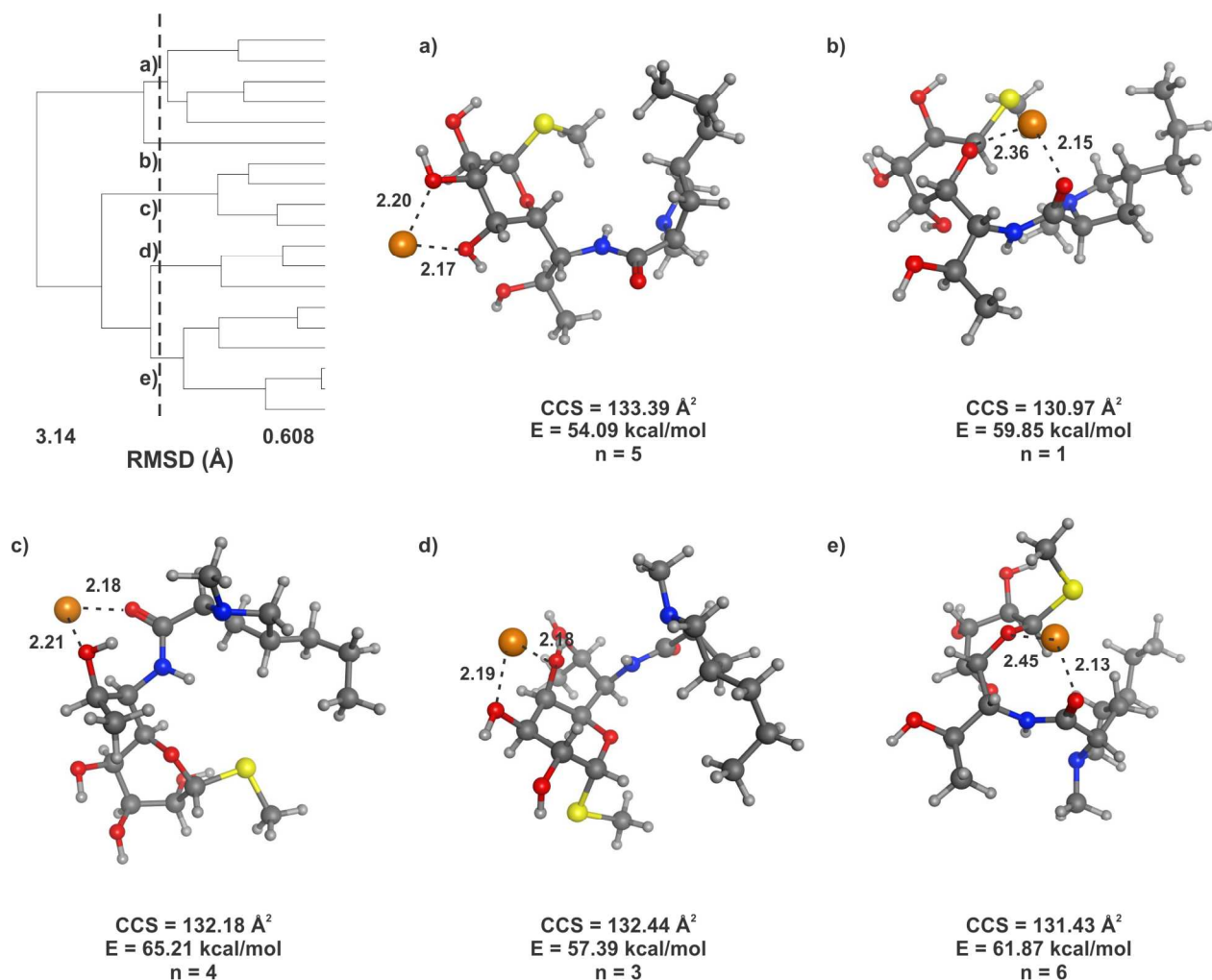


Figure S-22. Clustering analysis of 19 conformations of lincomycin generated with simulated annealing that fall within the experimental CCS range. Clustering is based on root mean square distance of atoms of superimposed structures. The vertical bar indicates the RMSD cutoff (2.10 Å) used to select the shown conformations. The conformations indicated on the clustering tree are shown with corresponding letters. Carbon atoms are shown in dark grey, hydrogen in light grey, oxygen in red, nitrogen in blue, sulfur in yellow, and sodium in orange. Each conformation is labeled with its theoretical CCS value, its theoretical energy, and the number of conformations it represents from the clustering analysis.

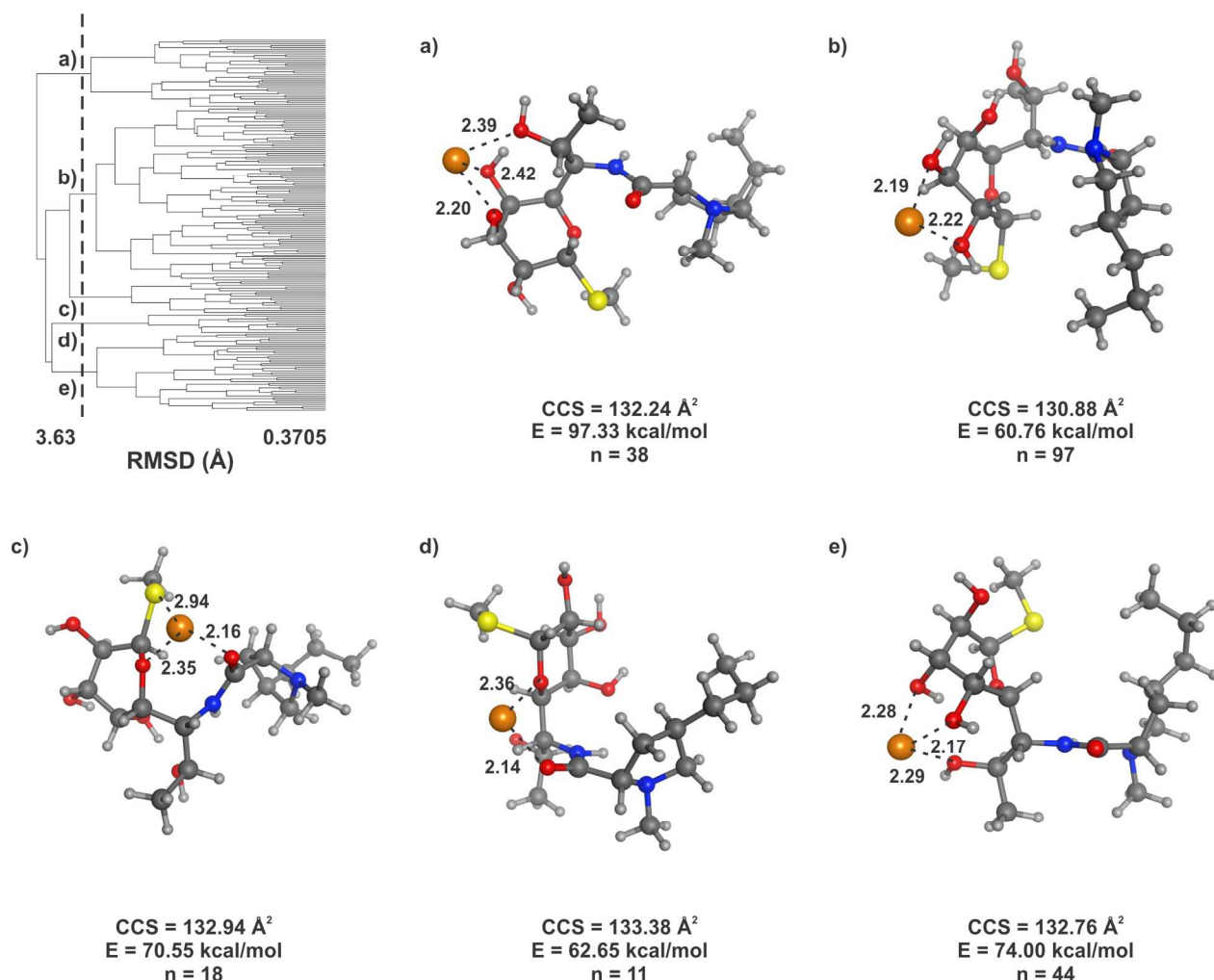


Figure S-23. Clustering analysis of 208 conformations of lincomycin generated with distance geometry and the molecular mechanics energy minimization that fall within the experimental CCS range. Clustering is based on root mean square distance of atoms of superimposed structures. The vertical bar indicates the RMSD cutoff (3.10 Å) used to select the shown conformations. The conformations indicated on the clustering tree are shown with corresponding letters. Carbon atoms are shown in dark grey, hydrogen in light grey, oxygen in red, nitrogen in blue, sulfur in yellow, and sodium in orange. Each conformation is labeled with its theoretical CCS value, its theoretical energy, and the number of conformations it represents from the clustering analysis.

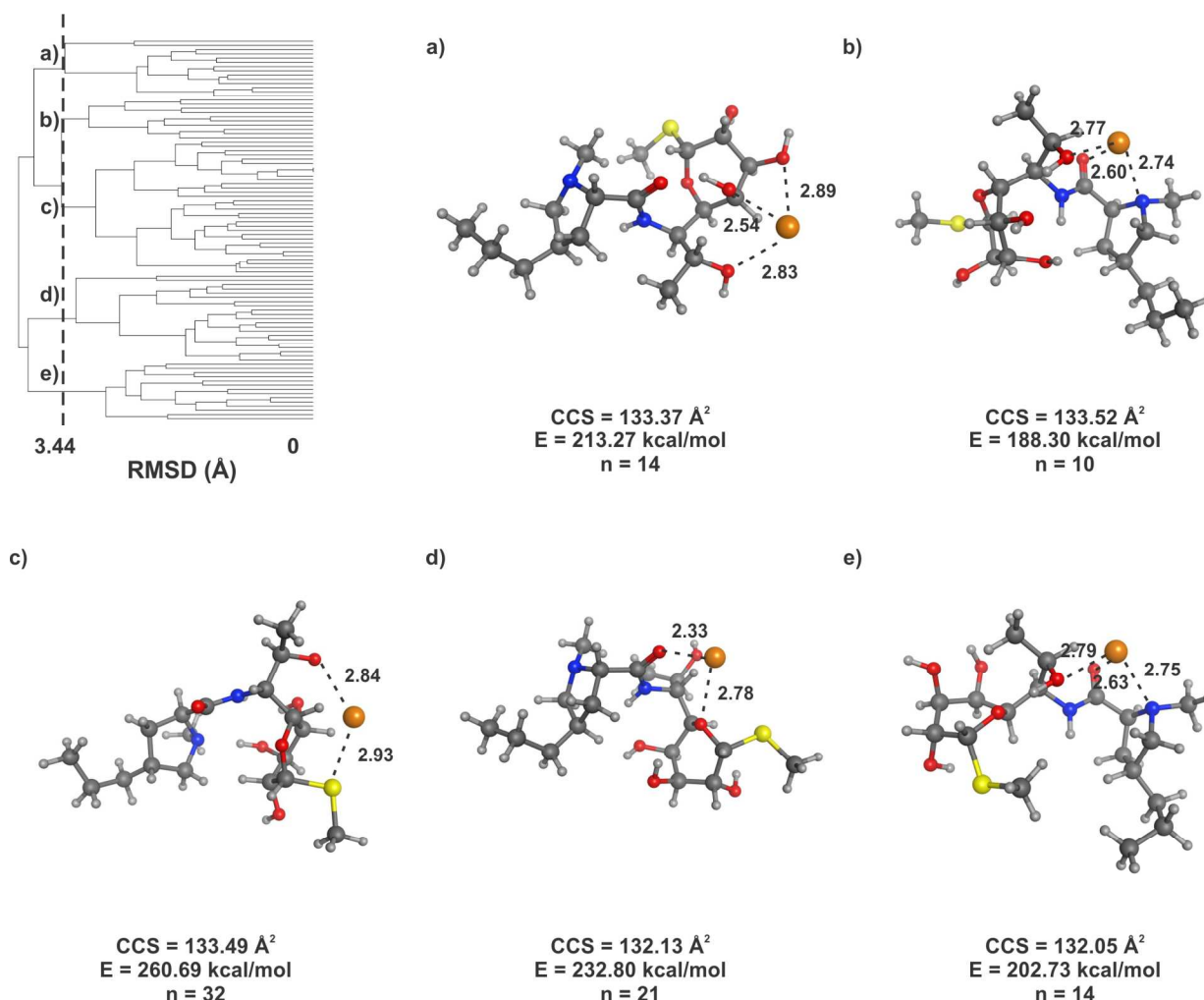


Figure S-24. Clustering analysis of 91 conformations of lincomycin generated with distance geometry and the QM geometry optimization that fall within the experimental CCS range. Clustering is based on root mean square distance of atoms of superimposed structures. The vertical bar indicates the RMSD cutoff (3.30 Å) used to select the shown conformations. The conformations indicated on the clustering tree are shown with corresponding letters. Carbon atoms are shown in dark grey, hydrogen in light grey, oxygen in red, nitrogen in blue, sulfur in yellow, and sodium in orange. Each conformation is labeled with its theoretical CCS value, its theoretical energy, and the number of conformations it represents from the clustering analysis.

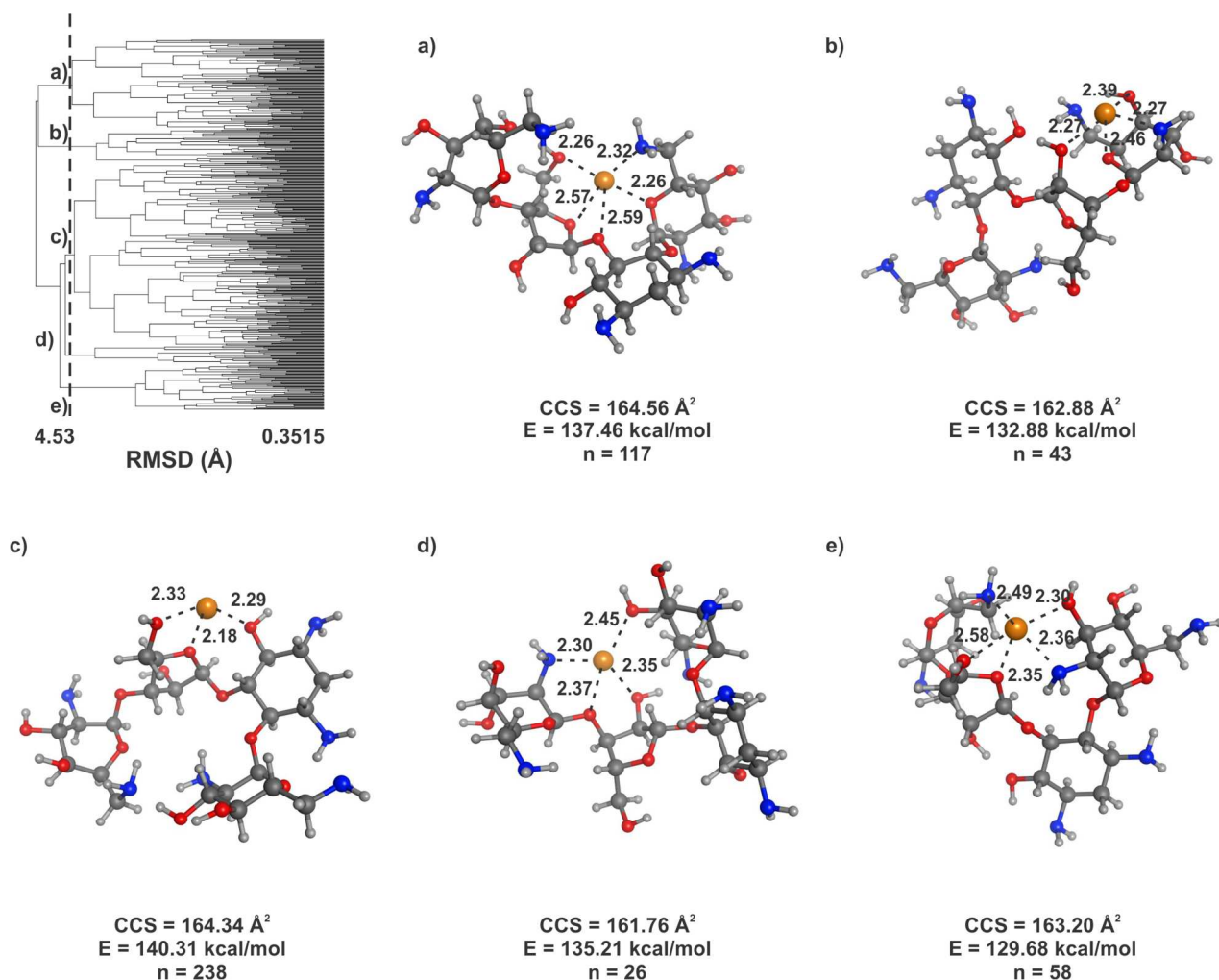


Figure S-25. Clustering analysis of 482 conformations of neomycin generated with simulated annealing that fall within the experimental CCS range. Clustering is based on root mean square distance of atoms of superimposed structures. The vertical bar indicates the RMSD cutoff (4.00 Å) used to select the shown conformations. The conformations indicated on the clustering tree are shown with corresponding letters. Carbon atoms are shown in dark grey, hydrogen in light grey, oxygen in red, nitrogen in blue, and sodium in orange. Each conformation is labeled with its theoretical CCS value, its theoretical energy, and the number of conformations it represents from the clustering analysis.

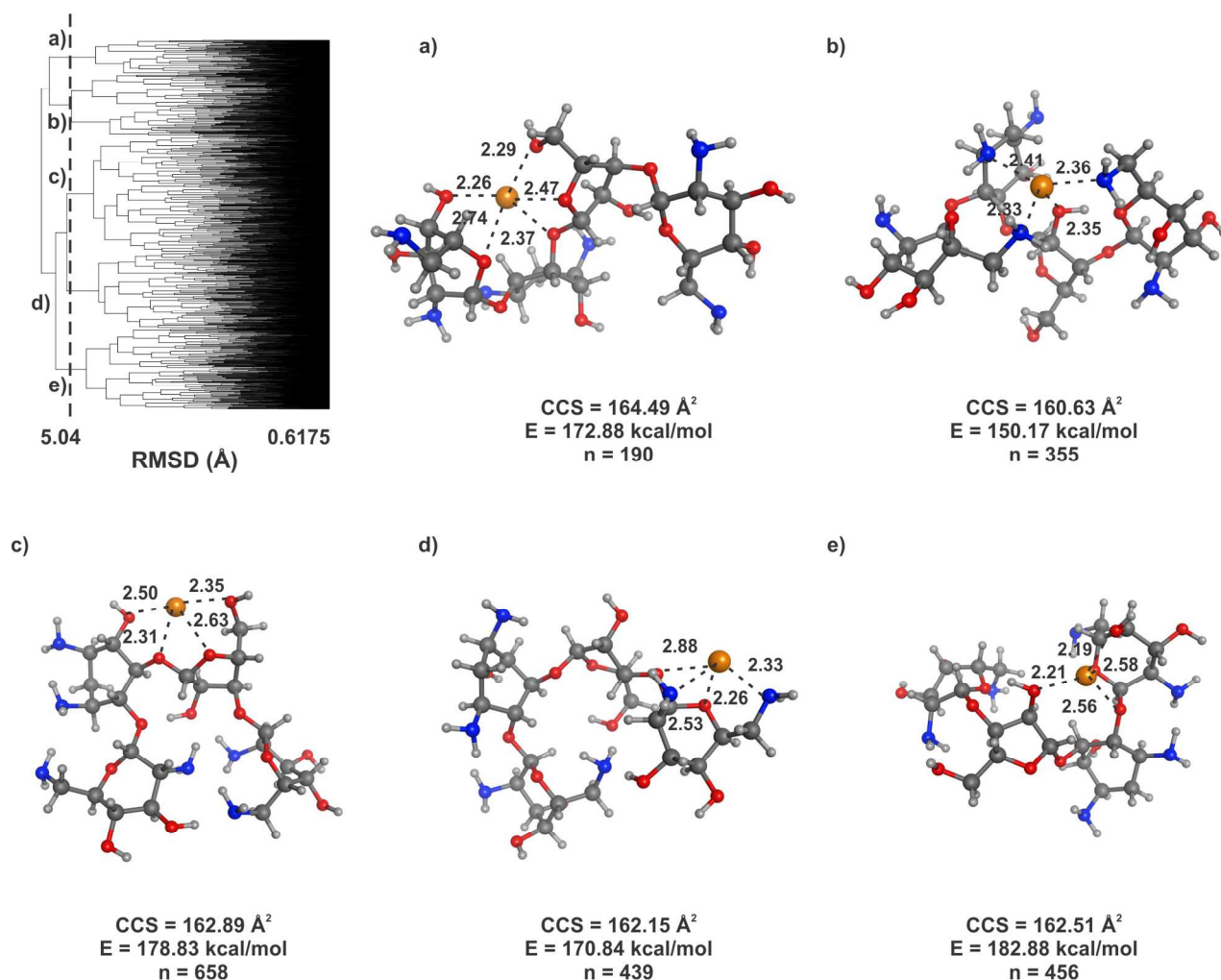


Figure S-26. Clustering analysis of 2098 conformations of neomycin generated with distance geometry and the molecular mechanics energy minimization that fall within the experimental CCS range. Clustering is based on root mean square distance of atoms of superimposed structures. The vertical bar indicates the RMSD cutoff (4.60 Å) used to select the shown conformations. The conformations indicated on the clustering tree are shown with corresponding letters. Carbon atoms are shown in dark grey, hydrogen in light grey, oxygen in red, nitrogen in blue, and sodium in orange. Each conformation is labeled with its theoretical CCS value, its theoretical energy, and the number of conformations it represents from the clustering analysis.

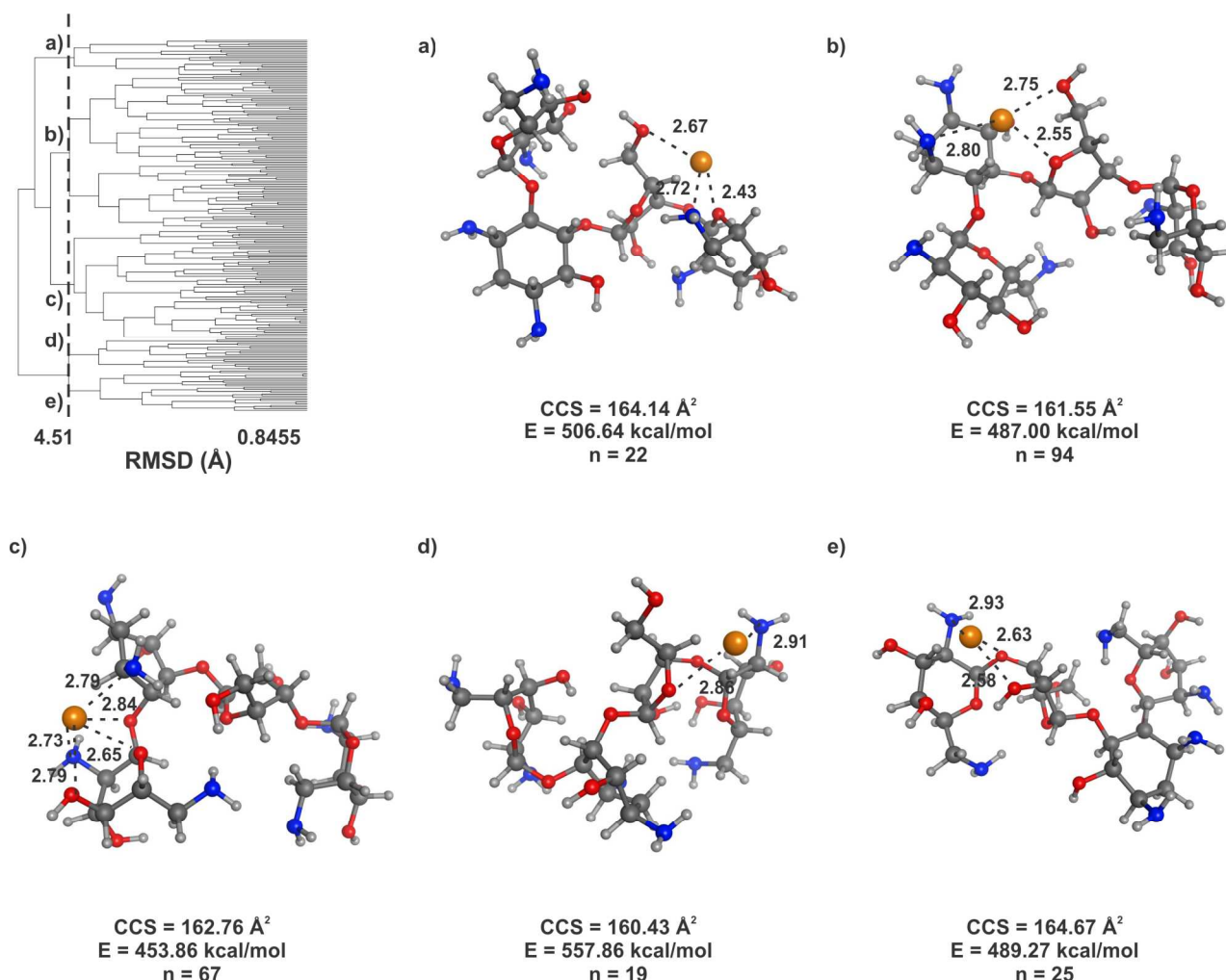


Figure S-27. Clustering analysis of 227 conformations of neomycin generated with distance geometry and the QM geometry optimization that fall within the experimental CCS range. Clustering is based on root mean square distance of atoms of superimposed structures. The vertical bar indicates the RMSD cutoff (3.86 Å) used to select the shown conformations. The conformations indicated on the clustering tree are shown with corresponding letters. Carbon atoms are shown in dark grey, hydrogen in light grey, oxygen in red, nitrogen in blue, and sodium in orange. Each conformation is labeled with its theoretical CCS value, its theoretical energy, and the number of conformations it represents from the clustering analysis.

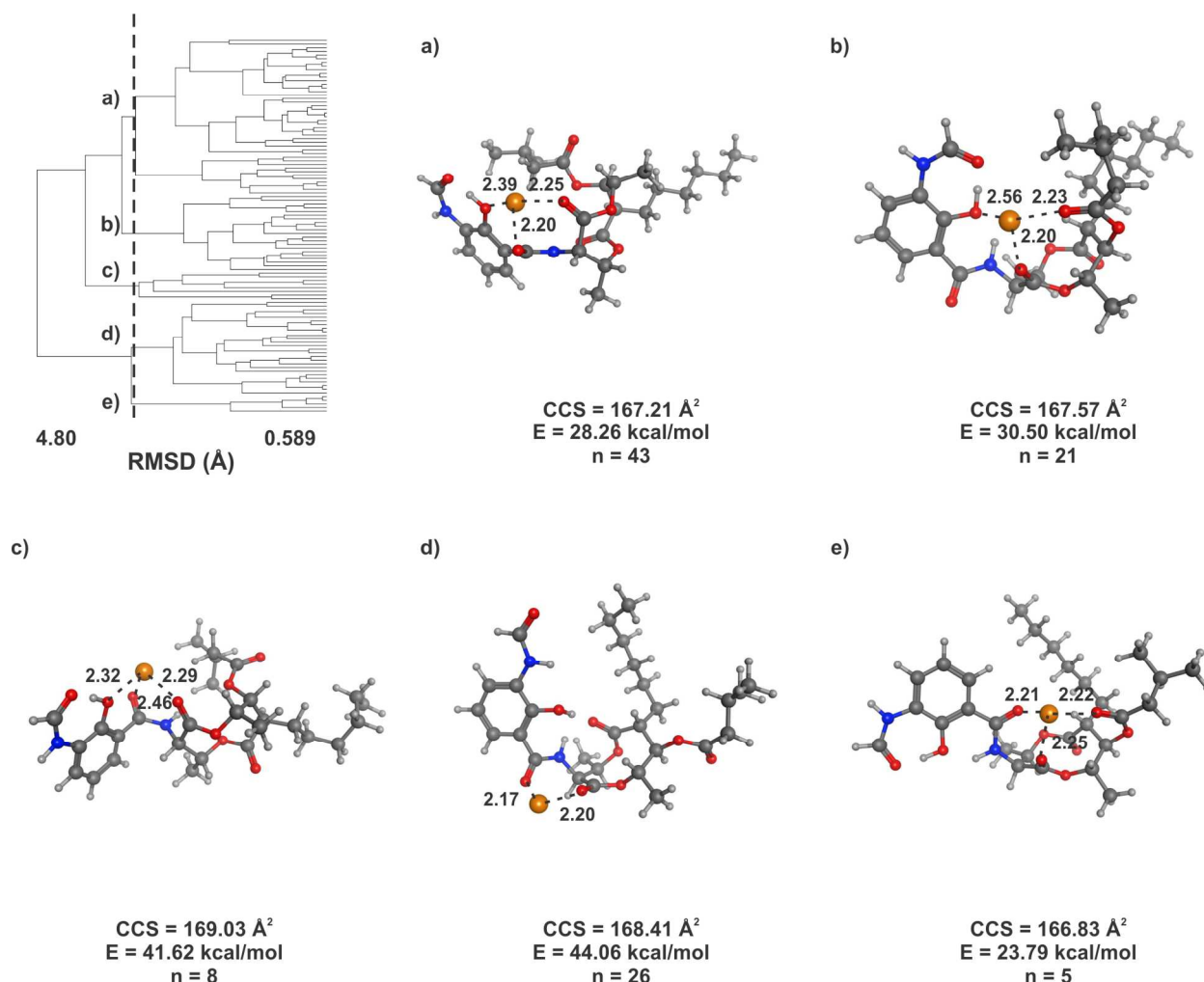


Figure S-28. Clustering analysis of 103 conformations of antimycin generated with simulated annealing that fall within the experimental CCS range. Clustering is based on root mean square distance of atoms of superimposed structures. The vertical bar indicates the RMSD cutoff (3.40 Å) used to select the shown conformations. The conformations indicated on the clustering tree are shown with corresponding letters. Carbon atoms are shown in dark grey, hydrogen in light grey, oxygen in red, nitrogen in blue, and sodium in orange. Each conformation is labeled with its theoretical CCS value, its theoretical energy, and the number of conformations it represents from the clustering analysis.

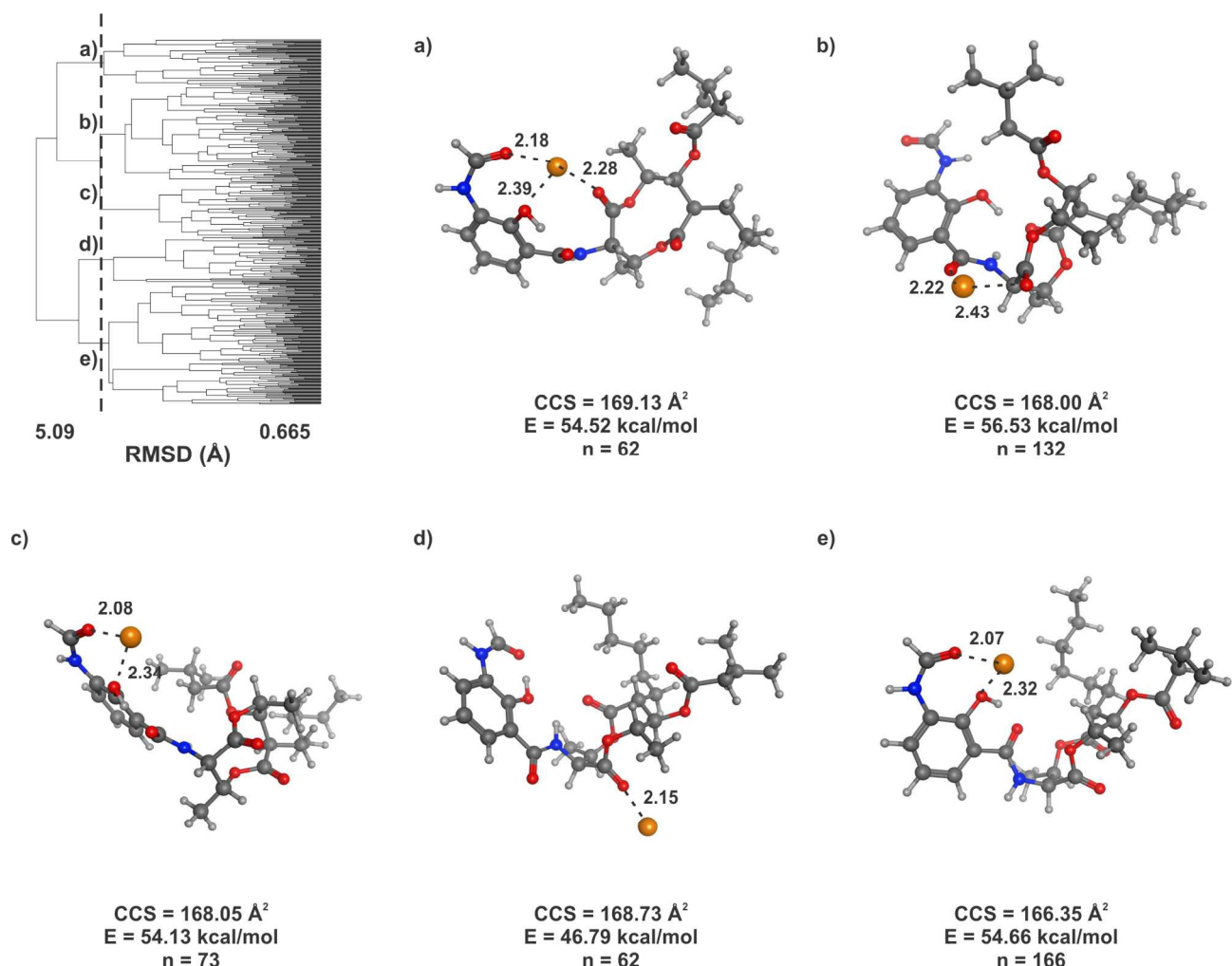


Figure S-29. Clustering analysis of 495 conformations of antimycin generated with distance geometry that fall within the experimental CCS range. Clustering is based on root mean square distance of atoms of superimposed structures. The vertical bar indicates the RMSD cutoff (4.05 Å) used to select the shown conformations. The conformations indicated on the clustering tree are shown with corresponding letters. Carbon atoms are shown in dark grey, hydrogen in light grey, oxygen in red, nitrogen in blue, and sodium in orange. Each conformation is labeled with its theoretical CCS value, its theoretical energy, and the number of conformations it represents from the clustering analysis.

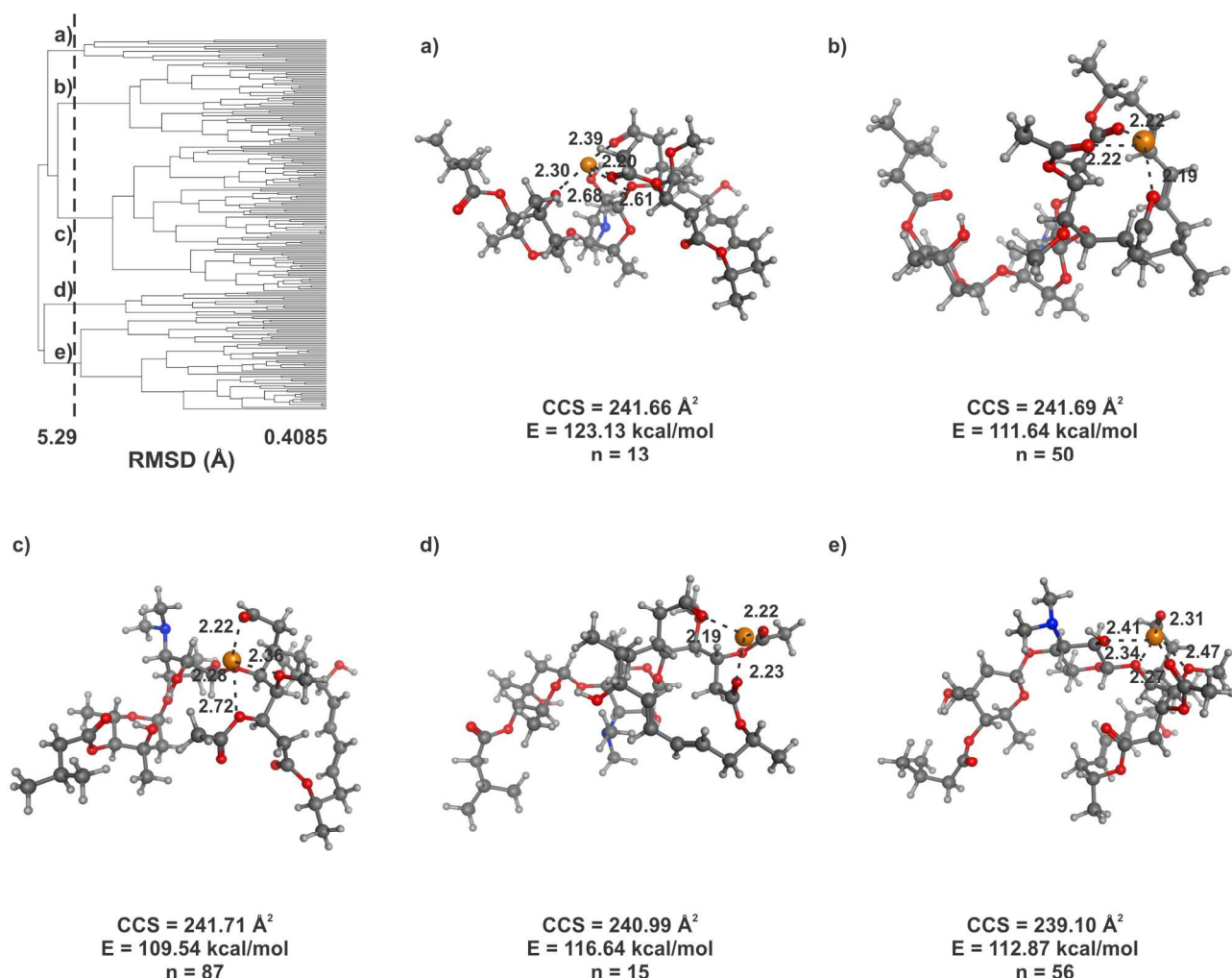


Figure S-30. Clustering analysis of 221 conformations of josamycin generated with simulated annealing that fall within the experimental CCS range. Clustering is based on root mean square distance of atoms of superimposed structures. The vertical bar indicates the RMSD cutoff (4.90 Å) used to select the shown conformations. The conformations indicated on the clustering tree are shown with corresponding letters. Carbon atoms are shown in dark grey, hydrogen in light grey, oxygen in red, nitrogen in blue, and sodium in orange. Each conformation is labeled with its theoretical CCS value, its theoretical energy, and the number of conformations it represents from the clustering analysis.

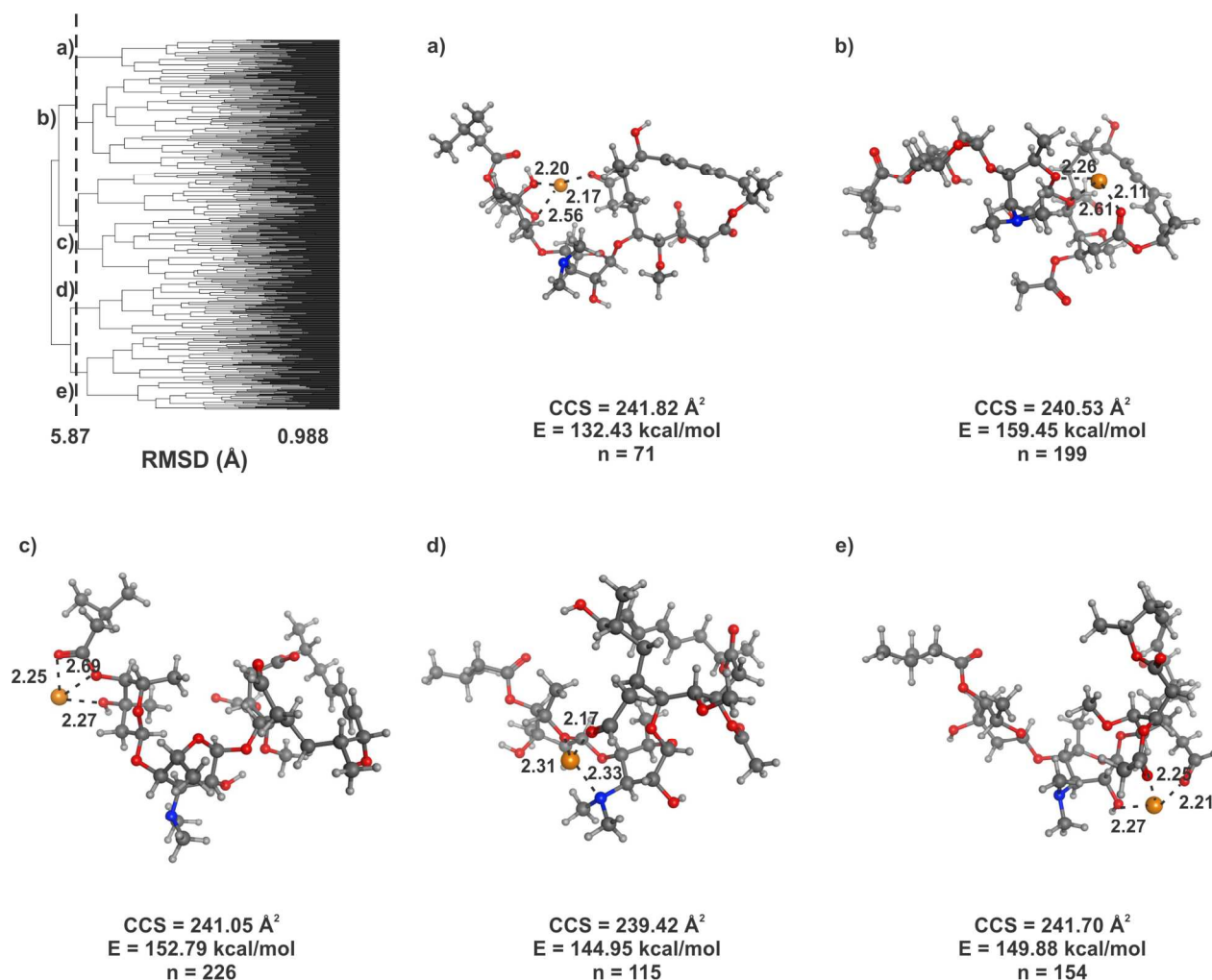


Figure S-31. Clustering analysis of 765 conformations of josamycin generated with distance geometry and the molecular mechanics energy minimization that fall within the experimental CCS range. Clustering is based on root mean square distance of atoms of superimposed structures. The vertical bar indicates the RMSD cutoff (5.45 Å) used to select the shown conformations. The conformations indicated on the clustering tree are shown with corresponding letters. Carbon atoms are shown in dark grey, hydrogen in light grey, oxygen in red, nitrogen in blue, and sodium in orange. Each conformation is labeled with its theoretical CCS value, its theoretical energy, and the number of conformations it represents from the clustering analysis.

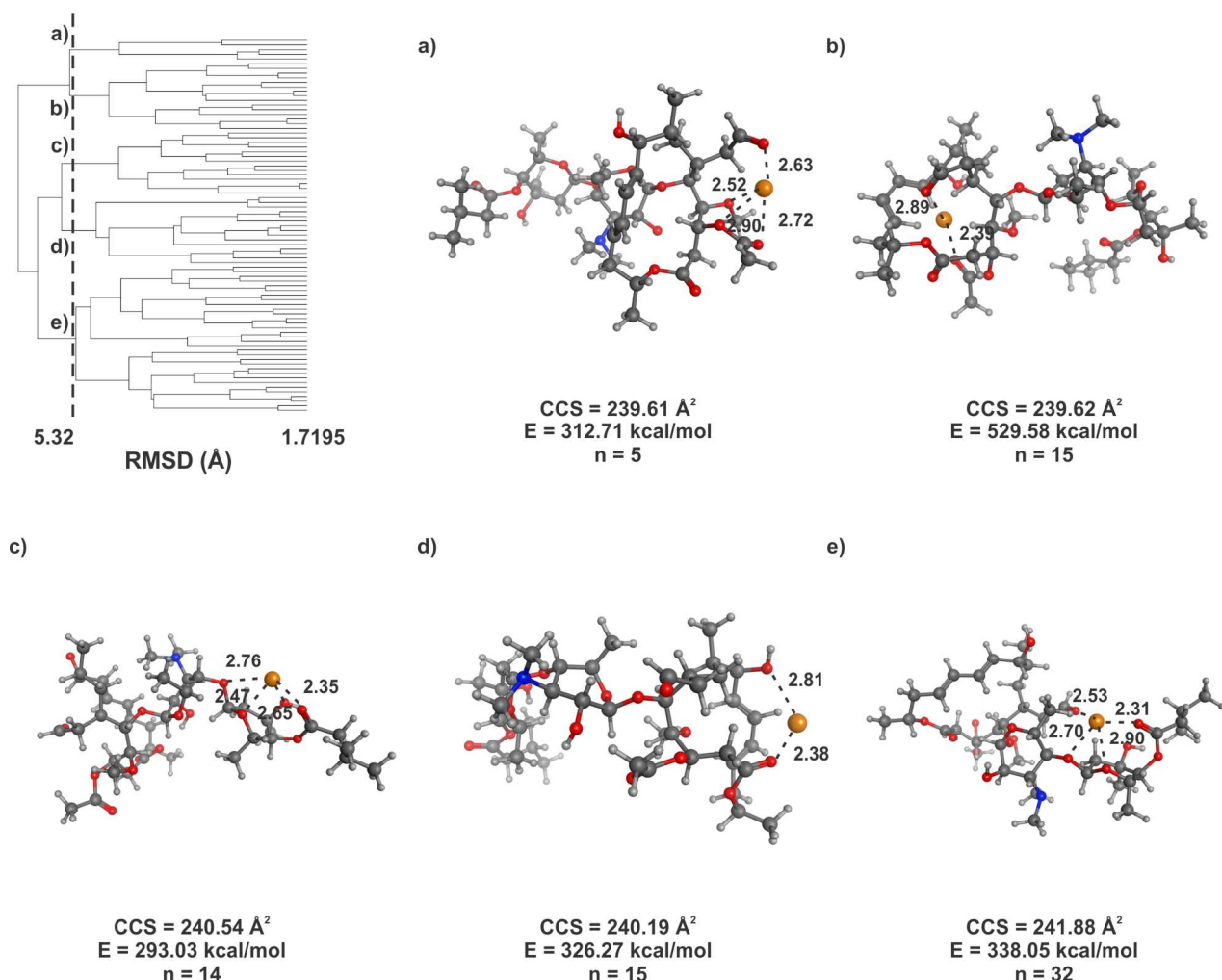


Figure S-32. Clustering analysis of 81 conformations of josamycin generated with distance geometry and the QM geometry optimization that fall within the experimental CCS range. Clustering is based on root mean square distance of atoms of superimposed structures. The vertical bar indicates the RMSD cutoff (4.60 Å) used to select the shown conformations. The conformations indicated on the clustering tree are shown with corresponding letters. Carbon atoms are shown in dark grey, hydrogen in light grey, oxygen in red, nitrogen in blue, and sodium in orange. Each conformation is labeled with its theoretical CCS value, its theoretical energy, and the number of conformations it represents from the clustering analysis.

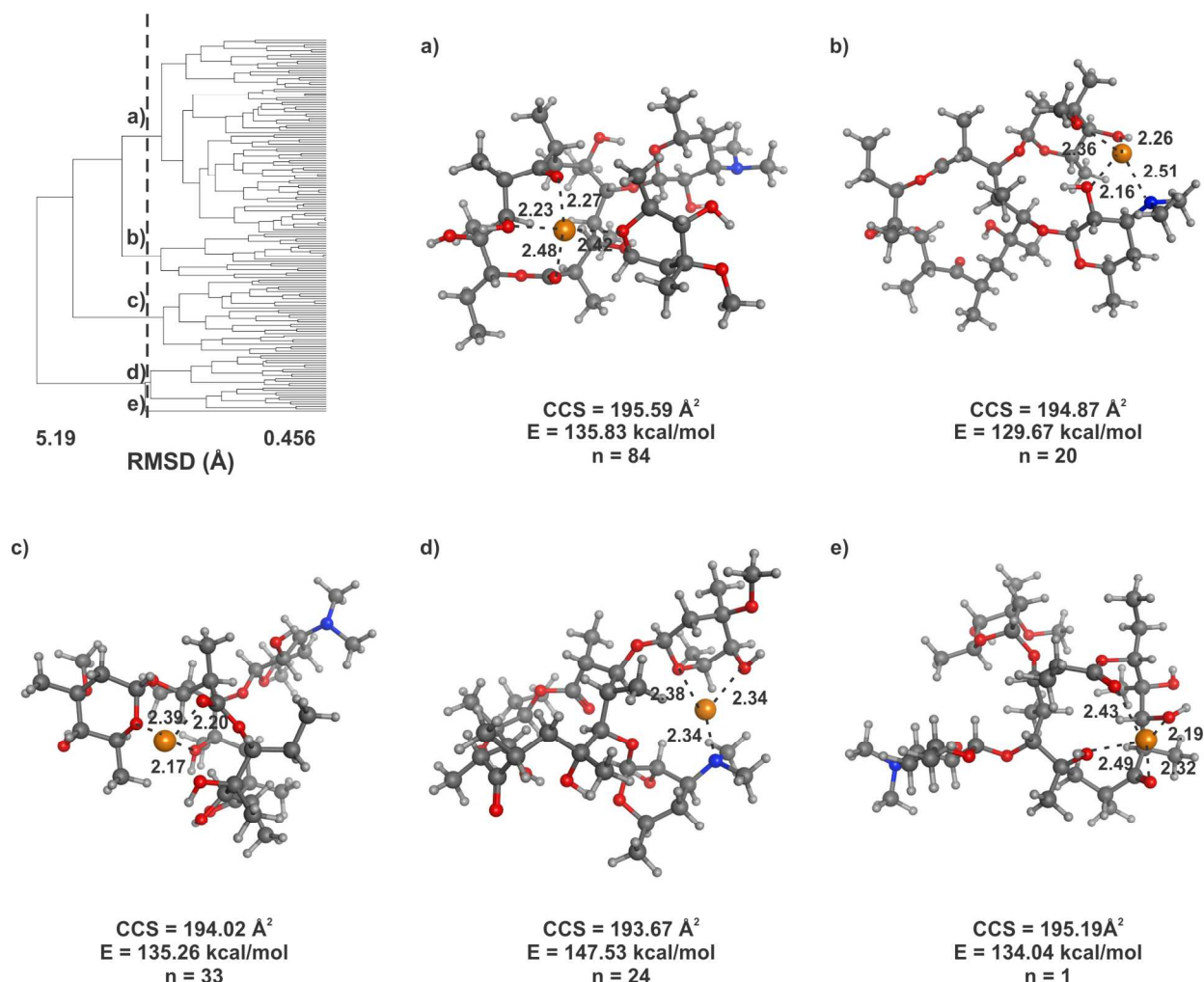


Figure S-33. Clustering analysis of 162 conformations of erythromycin generated with simulated annealing that fall within the experimental CCS range. Clustering is based on root mean square distance of atoms of superimposed structures. The vertical bar indicates the RMSD cutoff (3.40 Å) used to select the shown conformations. The conformations indicated on the clustering tree are shown with corresponding letters. Carbon atoms are shown in dark grey, hydrogen in light grey, oxygen in red, nitrogen in blue, and sodium in orange. Each conformation is labeled with its theoretical CCS value, its theoretical energy, and the number of conformations it represents from the clustering analysis.

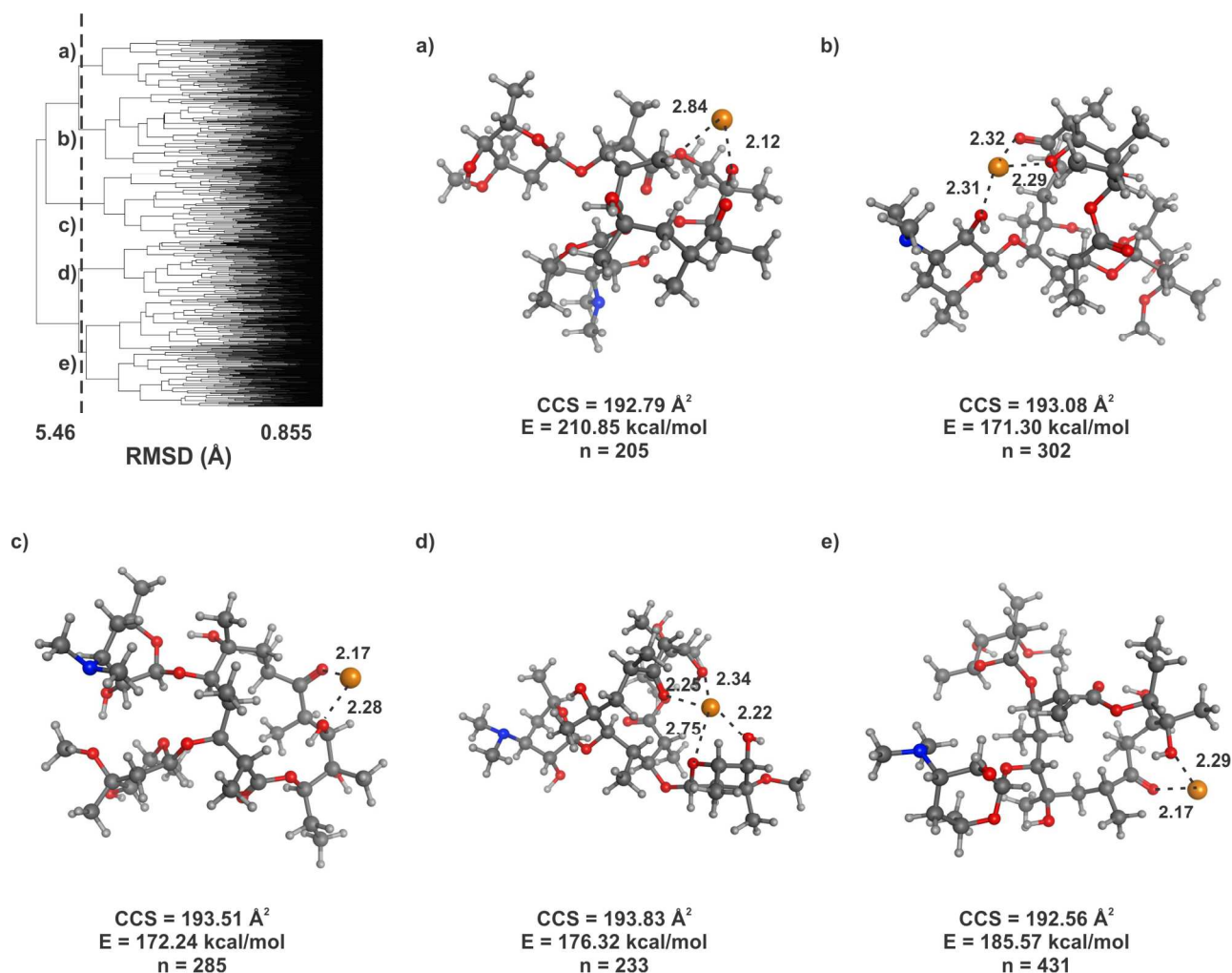


Figure S-34. Clustering analysis of 1456 conformations of erythromycin generated with distance geometry that fall within the experimental CCS range. Clustering is based on root mean square distance of atoms of superimposed structures. The vertical bar indicates the RMSD cutoff (4.70 Å) used to select the shown conformations. The conformations indicated on the clustering tree are shown with corresponding letters. Carbon atoms are shown in dark grey, hydrogen in light grey, oxygen in red, nitrogen in blue, and sodium in orange. Each conformation is labeled with its theoretical CCS value, its theoretical energy, and the number of conformations it represents from the clustering analysis.

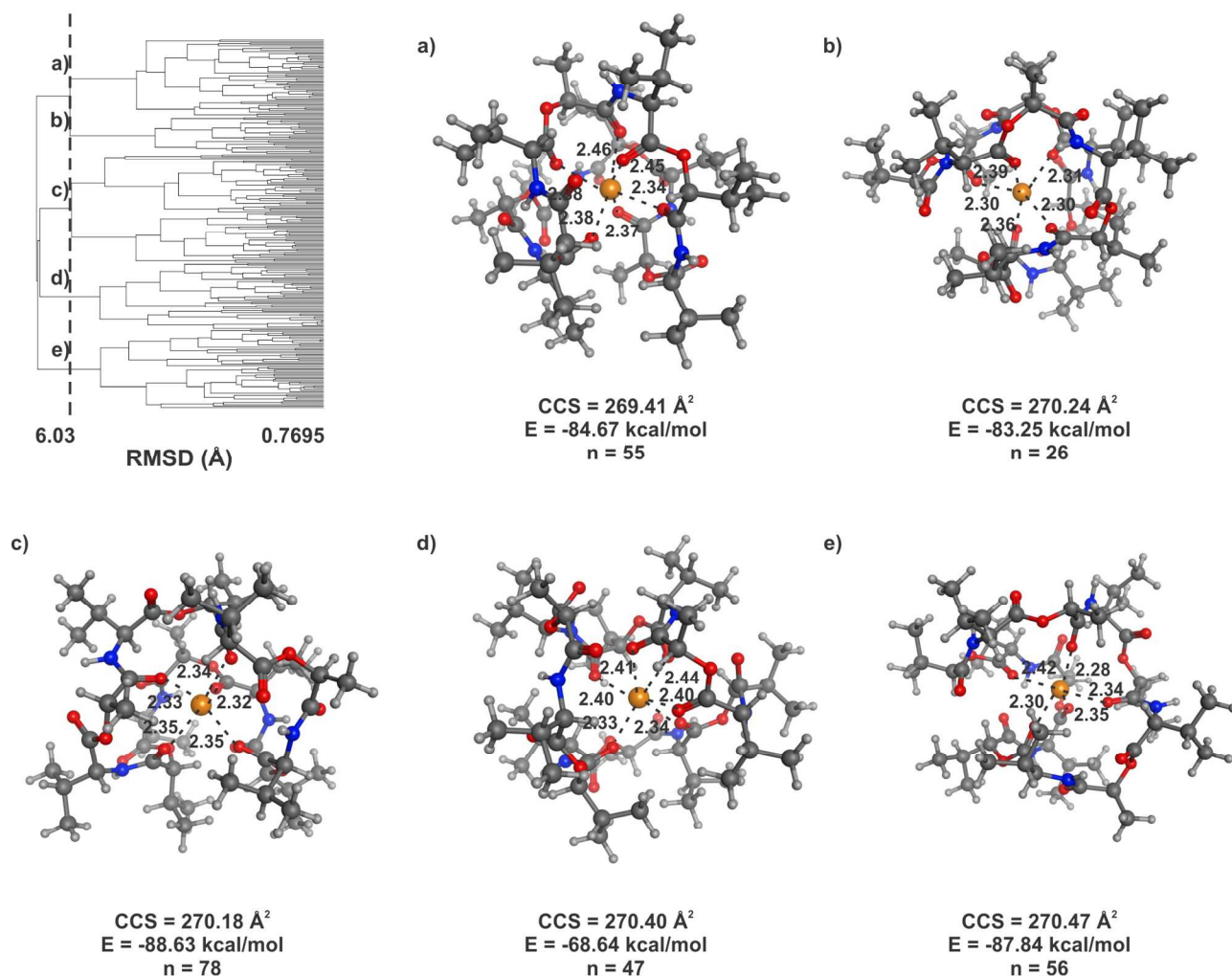


Figure S-35. Clustering analysis of 262 conformations of valinomycin generated with simulated annealing fall within the experimental CCS range. Clustering is based on root mean square distance of atoms of superimposed structures. The vertical bar indicates the RMSD cutoff (5.40 Å) used to select the shown conformations. The conformations indicated on the clustering tree are shown with corresponding letters. Carbon atoms are shown in dark grey, hydrogen in light grey, oxygen in red, nitrogen in blue, and sodium in orange. Each conformation is labeled with its theoretical CCS value, its theoretical energy, and the number of conformations it represents from the clustering analysis.

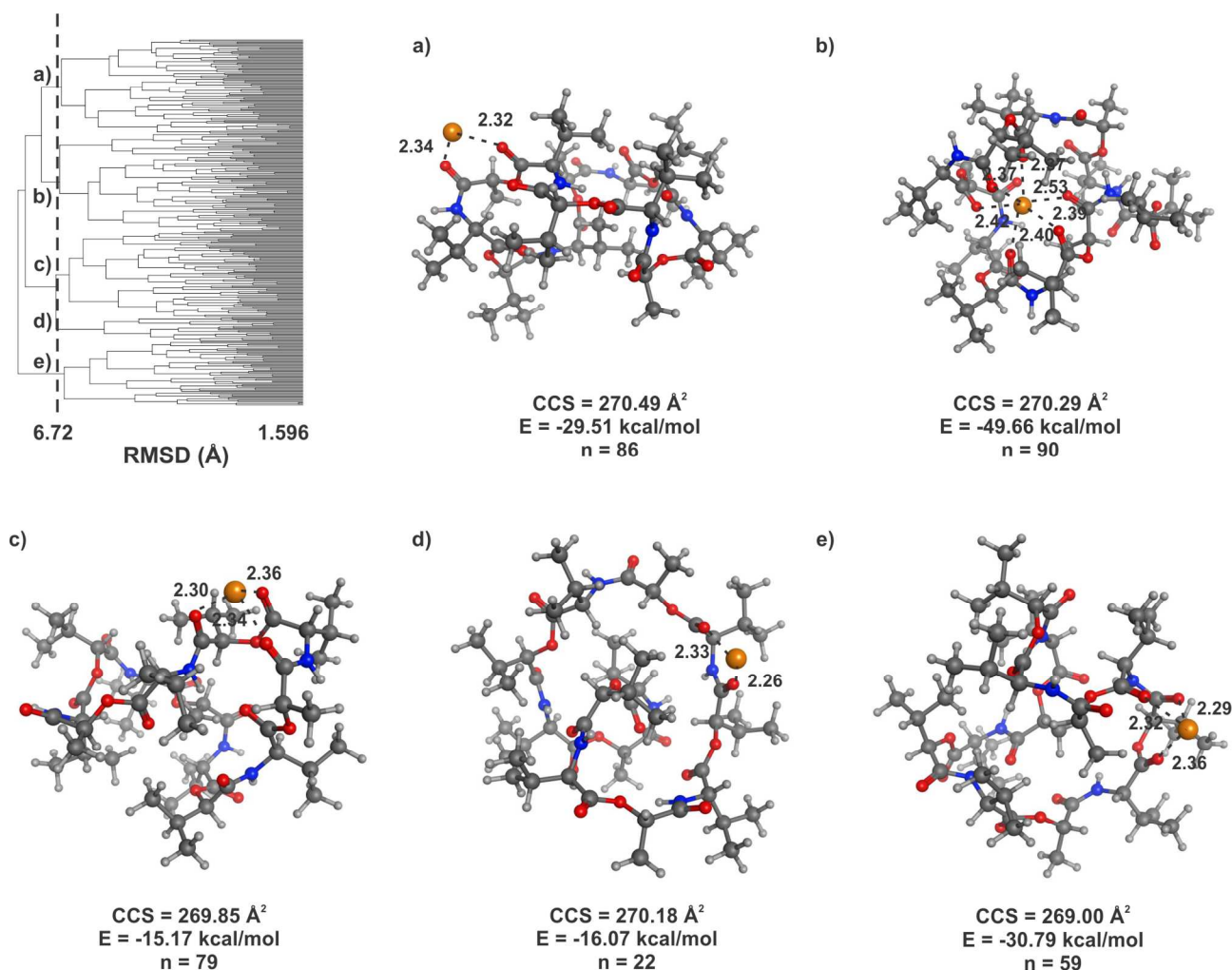


Figure S-36. Clustering analysis of 336 conformations of valinomycin generated with distance geometry that fall within the experimental CCS range. Clustering is based on root mean square distance of atoms of superimposed structures. The vertical bar indicates the RMSD cutoff (6.00 Å) used to select the shown conformations. The conformations indicated on the clustering tree are shown with corresponding letters. Carbon atoms are shown in dark grey, hydrogen in light grey, oxygen in red, nitrogen in blue, and sodium in orange. Each conformation is labeled with its theoretical CCS value, its theoretical energy, and the number of conformations it represents from the clustering analysis.

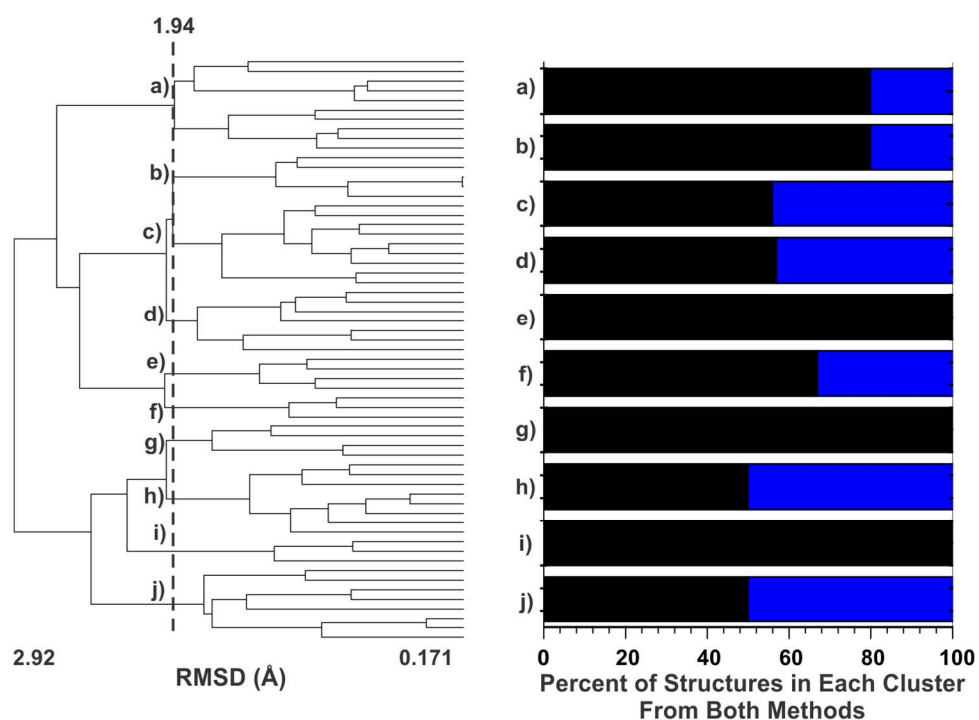


Figure S-37. Clustering analysis for the structures that align with the experimental CCS for doxorubicin from both distance geometry and simulated annealing. The structures are clustered into 10 unique clusters according to RMSD (1.94 Å) as indicated by the vertical dashed line on the cluster tree on the left. The percentage of conformations in each of the 10 clusters from either distance geometry (black) or simulated annealing (blue) is displayed in the histogram on the right.

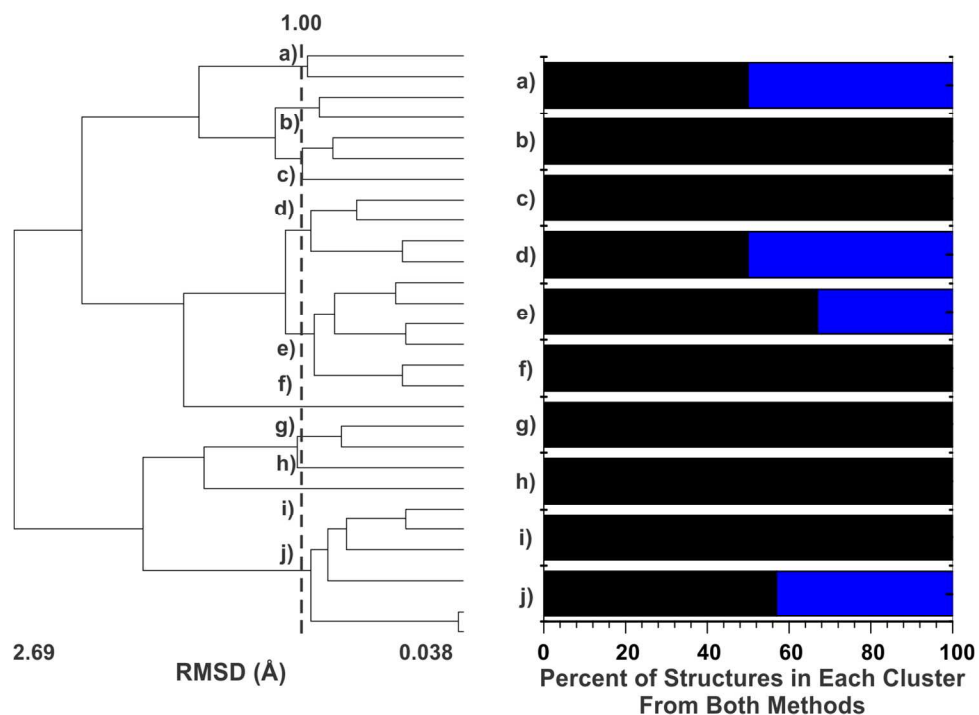


Figure S-38. Clustering analysis for the structures that align with the experimental CCS for capsaicin from both distance geometry and simulated annealing. The structures are clustered into 10 unique clusters according to RMSD (1.00 Å) as indicated by the vertical dashed line on the cluster tree on the left. The percentage of conformations in each of the 10 clusters from either distance geometry (black) or simulated annealing (blue) is displayed in the histogram on the right.

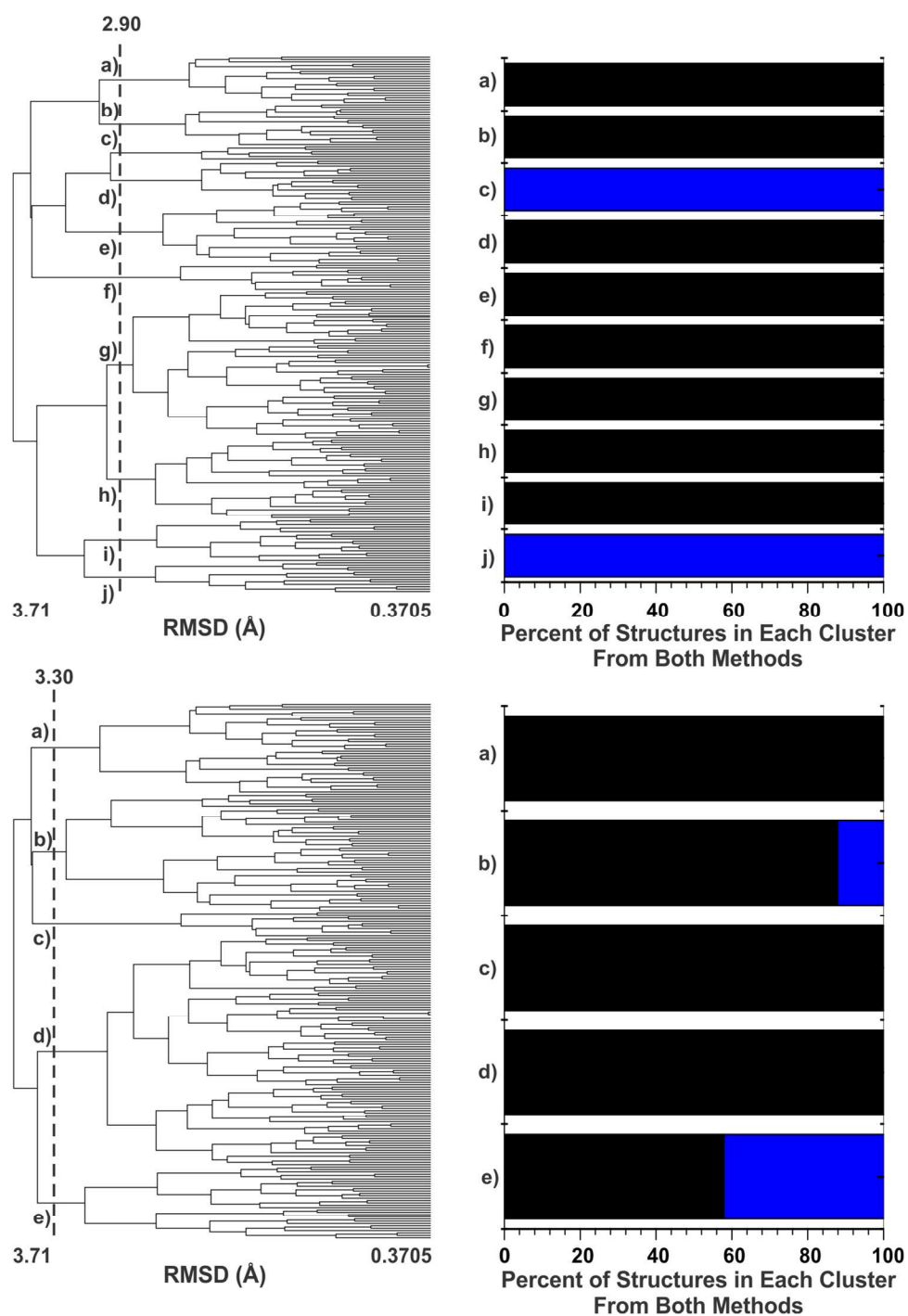


Figure S-39. Clustering analysis for the structures that align with the experimental CCS for lincomycin from both distance geometry and simulated annealing. The structures are clustered into both 10 and 5 unique clusters according to RMSD (2.90 and 3.30 Å) as indicated by the vertical dashed line on the cluster trees on the left. The percentage of conformations in each of the 10 or 5 clusters from either distance geometry (black) or simulated annealing (blue) is displayed in the histogram on the right. Analysis was performed on both 10 and 5 clusters to achieve structures from both methods in the same RMSD cluster.

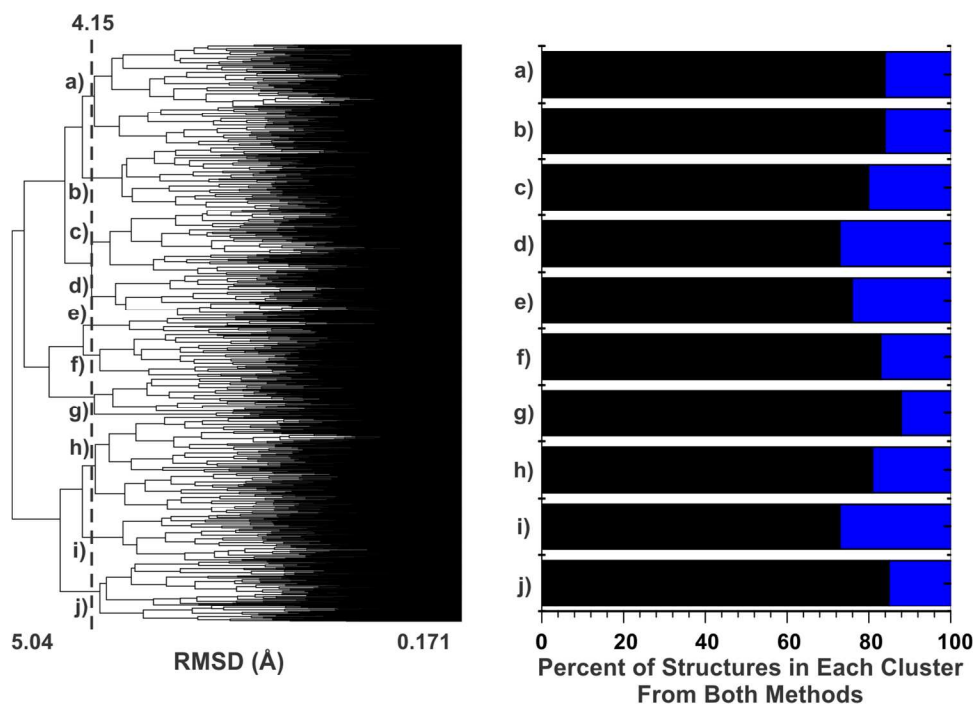


Figure S-40. Clustering analysis for the structures that align with the experimental CCS for neomycin from both distance geometry and simulated annealing. The structures are clustered into 10 unique clusters according to RMSD (4.15 Å) as indicated by the vertical dashed line on the cluster tree on the left. The percentage of conformations in each of the 10 clusters from either distance geometry (black) or simulated annealing (blue) is displayed in the histogram on the right.

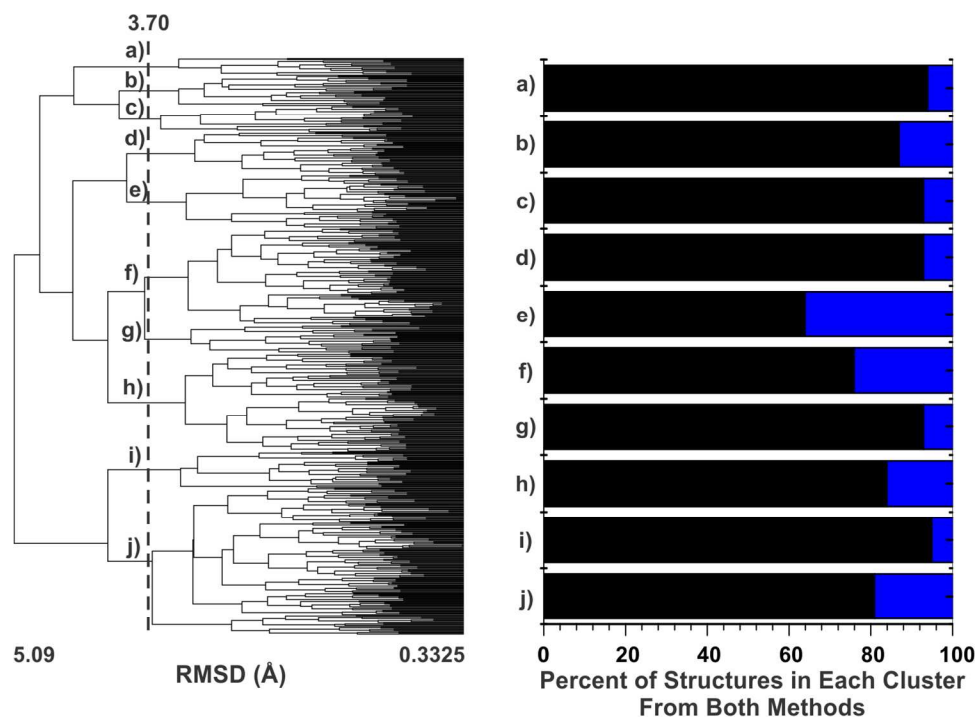


Figure S-41. Clustering analysis for the structures that align with the experimental CCS for antimycin from both distance geometry and simulated annealing. The structures are clustered into 10 unique clusters according to RMSD (3.70 Å) as indicated by the vertical dashed line on the cluster tree on the left. The percentage of conformations in each of the 10 clusters from either distance geometry (black) or simulated annealing (blue) is displayed in the histogram on the right.

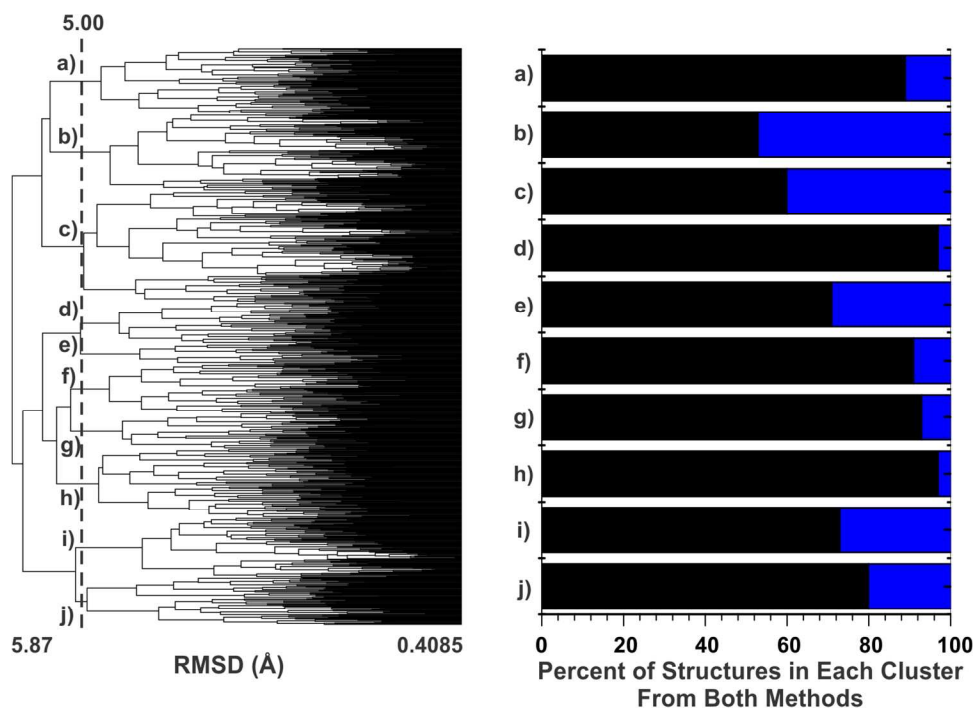


Figure S-42. Clustering analysis for the structures that align with the experimental CCS for josamycin from both distance geometry and simulated annealing. The structures are clustered into 10 unique clusters according to RMSD (5.00 Å) as indicated by the vertical dashed line on the cluster tree on the left. The percentage of conformations in each of the 10 clusters from either distance geometry (black) or simulated annealing (blue) is displayed in the histogram on the right.

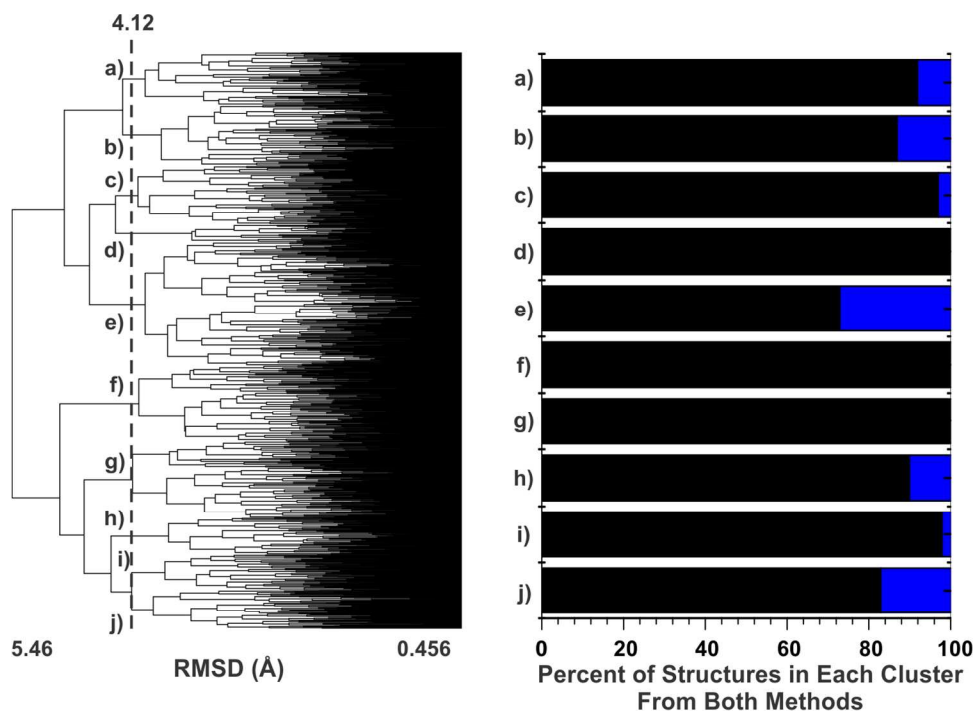


Figure S-43. Clustering analysis for the structures that align with the experimental CCS for erythromycin from both distance geometry and simulated annealing. The structures are clustered into 10 unique clusters according to RMSD (4.12 Å) as indicated by the vertical dashed line on the cluster tree on the left. The percentage of conformations in each of the 10 clusters from either distance geometry (black) or simulated annealing (blue) is displayed in the histogram on the right.

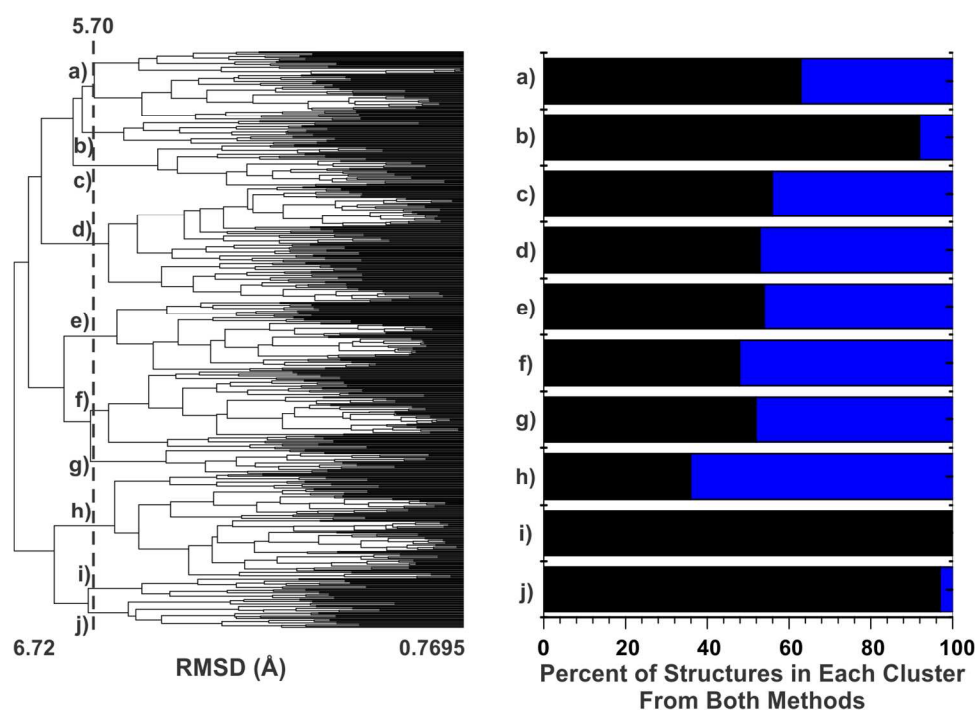


Figure S-44. Clustering analysis for the structures that align with the experimental CCS for valinomycin from both distance geometry and simulated annealing. The structures are clustered into 10 unique clusters according to RMSD (5.70 Å) as indicated by the vertical dashed line on the cluster tree on the left. The percentage of conformations in each of the 10 clusters from either distance geometry (black) or simulated annealing (blue) is displayed in the histogram on the right.